NASA TM- 84635

NASA Technical Memorandum 84635

NASA-TM-84635 19830018573

# DETERMINATION OF STABILITY AND CONTROL PARAMETERS OF A GENERAL AVIATION AIRPLANE FROM FLIGHT DATA



IMRAN ABBASY

MARCH 1983



NASA
National Aeronautics and
Space Administration

**Langley Research Center**
Hampton, Virginia 23665

# SUMMARY

Values for the stability and control derivatives of a single-engine, low-wing, general aviation airplane have been determined from flight data. Lateral and longitudinal transient maneuvers were analyzed by the equation error and output error methods. One quasi-steady maneuver was also investigated. An angle of attack range between 4 and 26 degrees was covered and there was a good agreement between the parameters extracted from flight data and those predicted by wind tunnel.

# INTRODUCTION

There have been a number of previous attempts to determine stability and control parameters from flight data. Gerlach and Howard in references 1 and 2 have applied the equation error method for the determination of longitudinal and lateral parameters, respectively. In references 3 and 4, parameters estimated from the output error method were compared with derivatives obtained from the wind tunnel and theoretical predictions. The parameter estimation problem is reasonably routine in flight conditions for which the aerodynamics are linearly related to the response and input variables. However, problems persist for the modeling of unsteady and high angles of attack aerodynamics. Most of the recent research effort has, therefore, been directed primarily towards these unresolved problems (refs. 5 to 11). Even though the problem of parameter estimation at low angles of attack has been well addressed in the past years, there have not been many applications in high angle of attack regimes. Furthermore, few attempts have been made to correlate the parameters extracted from flight data to the wind tunnel and theoretical predictions.

This work was done under the General Aviation Stall/Spin Program at NASA Langley Research Center. The primary objectives of this program were to gain a better understanding of the aerodynamics in pre- and post-stall regimes and to design and validate airframe modifications to improve stall/spin characteristics. Part of the overall program was devoted to the measurement of the airplane transient maneuvers for the subsequent extraction of the stability and control derivatives. The test airplane which produced the data for this analysis was tested with several modifications both in flight and in the wind tunnel. For the purpose of this report, data from only one of these modifications was used. In flight the airplane was excited from steady state flight at different airspeeds by conventional control surfaces, so that the entire operating angle of attack range was covered. The mathematical model was so postulated as to include nonlinear contributions to the equations of motion at high angles of attack.

The purpose of this report is to estimate the aerodynamic parameters from flight data covering angles of attack between 4 and 26 degrees, and to compare these parameters with those estimated from the static and oscillatory wind-tunnel tests. Also the validity of the parameters is checked by comparing the simulated data which is generated from the estimated model with the actual flight records. The estimation in this report was done by the stepwise regression method. Experience has shown that the stepwise regression and maximum likelihood methods give similar results. Therefore, only a few runs were analyzed by the maximum likelihood method to check the regression estimates.

## SYMBOLS

| | |
|---|---|
| $A$ | defined in Appendix B |
| $a_X$ | longitudinal acceleration, g units |
| $a_Y$ | lateral acceleration, g units |
| $a_Z$ | vertical acceleration, g units |
| $b$ | span, m |
| $C_A$ | axial-force coefficient, $-F_X/\bar{q}s$ |
| $C_D$ | drag coefficient, $D/\bar{q}s$ |
| $C_L$ | lift coefficient, $L/\bar{q}s$ |
| $C_\ell$ | rolling-moment coefficient, $M_X/\bar{q}Sb$ |
| $C_m$ | pitching-moment coefficient, $M_Y/\bar{q}S\bar{c}$ |
| $C_n$ | yawing-moment coefficient, $M_Z/\bar{q}Sb$ |
| $C_N$ | normal-force coefficient, $-F_Z/\bar{q}S$ |
| $C_T$ | thrust coefficient, $T/\bar{q}S$ |
| $C_X$ | longitudinal-force coefficient, $F_X/\bar{q}S$ |
| $C_Y$ | side-force coefficient, $F_Y/\bar{q}S$ |
| $C_Z$ | vertical-force coefficient, $F_Z/\bar{q}S$ |
| $\bar{c}$ | mean aerodynamic chord, m |
| $D$ | drag, N |
| $F_X,F_Y,F_Z$ | force along X, Y, and Z body axis, respectively, N |
| $G$ | airplane response vector |
| $g$ | acceleration due to gravity, m/sec$^2$ |
| $h$ | distance of CG aft of leading edge of wing, percent of $\bar{c}$ |
| $I_X,I_Y,I_Z$ | moment of inertia about X, Y, and Z body axis, respectively kg-m$^2$ |
| $I_{XZ}$ | product of inertia, kg-m$^2$ |
| $J$ | cost function |
| $k$ | normalized frequency, $\omega\bar{c}/2V$ or $\omega b/2V$ |
| $L$ | lift, N |
| $M_X,M_Y,M_Z$ | moment about X, Y, and Z body axis, respectively, N-m |
| $m$ | mass, kg |
| $N$ | number of data points |
| $p$ | body axis roll rate, rad/sec |
| $q$ | body axis pitch rate, rad/sec |
| $\bar{q}$ | dynamic pressure, $1/2\rho V^2$ |

| | |
|---|---|
| $R^{-1}$ | weighting matrix |
| $r$ | body axis yaw rate, rad/sec |
| $S$ | wing area, $m^2$ |
| $T$ | thrust, N |
| $u,v,w$ | velocity along X, Y, and Z body axis, respectively, m/sec |
| $V$ | airplane total velocity, m/sec |
| $y$ | aerodynamic force or moment coefficient |
| $\alpha$ | angle of attack, rad or deg |
| $\beta$ | angle of sideslip, rad |
| $\delta$ | defined in Appendix B |
| $\delta_a$ | aileron deflection, rad |
| $\delta_e$ | elevator deflection, rad |
| $\delta_r$ | rudder deflection, rad |
| $\varepsilon$ | thrust vector angle with respect to longitudinal body axis, rad |
| $\Theta$ | stability and control derivative vector |
| $\theta$ | pitch angle, rad |
| $\rho$ | air density, $kg/m^3$ |
| $\phi$ | roll angle, rad |
| $\psi$ | yaw angle, rad |
| $\omega$ | frequency, rad/sec |

Subscripts:

| | |
|---|---|
| o | trim value |
| M | measured value |
| WT | wind tunnel |

Superscripts:

| | |
|---|---|
| T | transpose |
| $\cdot$ | derivative with respect to time |
| ' | derivatives defined in Appendices A and B |
| ^ | estimate |

Abbreviations:

| | |
|---|---|
| CG | center of gravity |
| ML | maximum likelihood |
| SR | stepwise regression |

Derivatives:

$$C_{A_q} = \frac{\partial C_A}{\partial q\bar{c}/2V} \qquad C_{A_{\dot{\alpha}}} = \frac{\partial C_A}{\partial \dot{\alpha}\bar{c}/2V} \qquad C_{D_\alpha} = \frac{\partial C_D}{\partial \alpha}$$

$$C_{D_{\delta_e}} = \frac{\partial C_D}{\partial \delta_e} \qquad C_{L_\alpha} = \frac{\partial C_L}{\partial \alpha} \qquad C_{L_{\delta_e}} = \frac{\partial C_L}{\partial \delta_e}$$

$$C_{N_q} = \frac{\partial C_N}{\partial q\bar{c}/2V} \qquad C_{N_{\dot{\alpha}}} = \frac{\partial C_N}{\partial \dot{\alpha}\bar{c}/2V}$$

$$C_{X_\alpha} = \frac{\partial C_X}{\partial \alpha} \qquad C_{X_q} = \frac{\partial C_X}{\partial q\bar{c}/2V} \qquad C_{X_{\delta_e}} = \frac{\partial C_X}{\partial \delta_e}$$

$$C_{Z_\alpha} = \frac{\partial C_Z}{\partial \alpha} \qquad C_{Z_q} = \frac{\partial C_Z}{\partial q\bar{c}/2V} \qquad C_{Z_{\delta_e}} = \frac{\partial C_Z}{\partial \delta_e}$$

$$C_{m_\alpha} = \frac{\partial C_m}{\partial \alpha} \qquad C_{m_q} = \frac{\partial C_m}{\partial q\bar{c}/2V} \qquad C_{m_{\delta_e}} = \frac{\partial C_m}{\partial \delta_e}$$

$$C_{Y_\beta} = \frac{\partial C_Y}{\partial \beta} \qquad C_{\ell_\beta} = \frac{\partial C_\ell}{\partial \beta} \qquad C_{n_\beta} = \frac{\partial C_n}{\partial \beta}$$

$$C_{Y_p} = \frac{\partial C_Y}{\partial pb/2V} \qquad C_{\ell_p} = \frac{\partial C_\ell}{\partial pb/2V} \qquad C_{n_p} = \frac{\partial C_n}{\partial pb/2V}$$

$$C_{Y_r} = \frac{\partial C_Y}{\partial rb/2V} \qquad C_{\ell_r} = \frac{\partial C_\ell}{\partial rb/2V} \qquad C_{n_r} = \frac{\partial C_n}{\partial rb/2V}$$

$$C_{Y_{\delta_a}} = \frac{\partial C_Y}{\partial \delta_a} \qquad C_{\ell_{\delta_a}} = \frac{\partial C_\ell}{\partial \delta_a} \qquad C_{n_{\delta_a}} = \frac{\partial C_n}{\partial \delta_a}$$

$$C_{Y_{\delta_r}} = \frac{\partial C_Y}{\partial \delta_r} \qquad C_{\ell_{\delta_r}} = \frac{\partial C_\ell}{\partial \delta_r} \qquad C_{n_{\delta_r}} = \frac{\partial C_n}{\partial \delta_r}$$

$$C_{Y_{\dot\beta}} = \frac{\partial C_Y}{\partial \dot\beta b/2V} \qquad C_{\ell_{\dot\beta}} = \frac{\partial C_\ell}{\partial \dot\beta b/2V} \qquad C_{n_{\dot\beta}} = \frac{\partial C_n}{\partial \dot\beta b/2V}$$

$$C_{m_{\dot\alpha}} = \frac{\partial C_m}{\partial \dot\alpha\bar{c}/2V} \qquad C_{X_{\alpha^2}} = \frac{1}{2}\,\frac{\partial^2 C_X}{\partial \alpha^2} \qquad C_{Z_{\alpha^2}} = \frac{1}{2}\,\frac{\partial^2 C_Z}{\partial \alpha^2}$$

$$C_{\ell_{\alpha^2\beta}} = \frac{1}{2}\,\frac{\partial^3 C_\ell}{\partial \alpha^2 \partial \beta}$$

## Flight Test and Data Reduction

A single-engine, low-wing, general aviation airplane with a fixed tricycle landing gear was used as the test vehicle. Since this airplane had been tested in spins, a spin recovery parachute system was installed. Furthermore, the configuration flight tested for parameter extraction had as an additional modification, an outboard leading edge droop, which enabled trimmed flight at high angles of attack. Figure 1 is a three view drawing of the test airplane and figure 2 is a drawing of the tested configuration. Table I lists the physical characteristics of the airplane. The flight data was recorded by an onboard instrumentation system, and was sampled at 40 cycles/sec. However, for the estimation purposes every other sample was used. For the longitudinal maneuvers, a simple elevator doublet or a combination of several doublets was chosen based upon reference 4. For lateral maneuvers the aileron and rudder inputs should have not only good harmonic content but also proper phase relationships. In accordance with the conclusions in reference 4, a rudder followed by aileron input or vice versa was chosen. Typical time histories for the transient longitudinal and lateral maneuvers are given in figures 3 and 4, respectively. In addition, one slow acceleration/deceleration run was also analyzed as quasi-steady maneuver, where airplane angle of attack is varied gradually by the elevator maintaining a constant pitch-rate.

The validity of the flight data was checked using the technique presented in reference 12, which gives a way of estimating the states via the aircraft kinematic equations. In case the integrated accelerations do not match with the flight data, appropriate biases are computed. Wherever needed such instrument biases and dynamics were taken into account. The measured angles of attack and sideslip were corrected for the upwash and sidewash. The measured velocity was corrected based upon the calibration derived from flying the test airplane over a measured ground trace. Since the equations of motion used in the analysis are referred to the airplane center of gravity, the data were transformed accordingly.

## Parameter Extraction Techniques

There are several methods for the estimation of airplane stability and control parameters. Their basic differences are in the optimization criteria and assumptions regarding external disturbances and the presence of measurement noise in the data. The well established methods for airplane parameter estimation are the equation error and maximum likelihood methods. The present report uses a stepwise regression method which is a version of the equation error method.

(a) Stepwise regression (SR): This method is outlined in reference 14. It is based on the minimization of the cost function

$$J(\Theta) = \sum_{i=1}^{N} \left[ y_{M_i} - y(\Theta)_i \right]^2 \qquad (1)$$

In the equation, $y_M$ is the aerodynamic force or moment coefficient based upon the measured states and $y(\Theta)$ is calculated from the estimated parameters ($\Theta$). The difference between stepwise regression and ordinary linear regression is in the capability of the first technique to select independent variables from a set of candidate parameters one at a time, until the regression is completed. The order of insertion and the adequacy of the model is determined by various statistical criteria. For a more detailed description the reader is referred to references 13, 14, and 15.

(b) Maximum likelihood (ML): This is a nonlinear estimation technique and therefore requires an iterative solution. The method minimizes the error between the measured and predicted outputs. For no process noise the simplified cost function that has to be minimized is

$$J(\Theta) = \sum_{i=1}^{N} \left[ G_{M_i} - G(\Theta)_i \right]^T R^{-1} \left[ G_{M_i} - G(\Theta)_i \right] \qquad (2)$$

where G is the airplane response vector, $[V\ \alpha\ q\ \theta]^T$ or $[\beta\ p\ r\ \phi]^T$, and $R^{-1}$ is the weighting matrix.

For a detailed discussion the reader is referred to references 13, 16, and 17.

Results and Discussion

There were 7 test flights for two CG locations, out of which a total of 62 longitudinal and 58 lateral maneuvers were available for analysis. In addition a total of 6 slow acceleration-deceleration runs for the two configurations were also made. The stepwise regression method was considered more suitable than the maximum likelihood method for the estimation due to its simplicity and its capability of selecting the appropriate model. Also, the low noise level on the data guaranteed the efficiency of the technique (ref. 10).

Typical results for the longitudinal and lateral modes are shown in Table II. Figure 5 illustrates an example of a regression model and the autocorrelation coefficient of the residuals of the computed and measured coefficients. The features to note are the reasonable fit for the computed and measured coefficients, and the rapidly falling autocorrelation of the residuals signifying a random sequence. The estimated parameters using two parameter estimation methods are shown in figures 6 through 13 for idle power conditions. The standard errors were under 10 percent for most of the parameters. The model determined was linear until about 10° angle of attack, and at higher angles of attack nonlinear terms (Appendix A) were also included. The nonlinear terms improved the fit to the data, but did not significantly change the values of the linear terms. Since different nonlinear terms were selected as being siginificant for each parameter extraction run, no attempt has been made to document them. The figures also show the repeatability of results from various flights and their consistency with the ML estimates. Some maneuvers for different power settings were also available, but the data were insufficient to make any useful observations.

The acceleration/deceleration run was analyzed assuming quasi-steady flight (constant pitch-rate). Using the known elevator effectiveness, the effect of the elevator was removed to obtain the aerodynamic coefficients as a function of only angle of attack. Figure 14 shows a good agreement between the wind tunnel and flight determined $C_L$ and $C_m$.

Figures 15 through 22 give a comparison of the parameters estimated from flight using the SR method and the wind tunnel predictions.

1. Longitudinal Parameters:

The X-force derivatives generally had higher standard errors (10 to 50 percent) and had a poor comparison with the wind-tunnel results, as shown in figure 15. This is attributed to thrust effects (i.e., idle power is not necessarily zero thrust) and the lack of excitation of this mode. A definite trend is apparent until about 12° angle of attack, and a scatter is observed for higher angles of attack.

The Z-force derivatives were well defined (standard error less than 5 percent) and the static derivatives showed good agreement with the wind-tunnel estimates (Figure 16). $C_{Z_q}$, however, did not agree with the wind tunnel, which predicts a positive trend in the parameter. A study of the aerodynamic characteristics of general aviation airplanes in the same class substantiated the results obtained from flight (reference 18). The unusual contradiction between the flight and wind tunnel estimates has not been explained.

The pitching moment derivatives were generally of low standard error (less than 5 percent) and distinct trends with respect to angle of attack were observed, as shown in Figure 17. Though the configuration flight tested had different CG locations, the flight estimates failed to separate the respective $C'_{m_\alpha}$ s (figure 8). An attempt to separate the $C'_{m_\alpha}$ s was made using the ML method, but there was no significant change. Overall, the trends between the flight and wind tunnel $C'_{m_\alpha}$ s agreed very well. $C'_{m_q}$ was harder to estimate due to the high correlation with $C'_{m_{\delta_e}}$, as was shown by the ML technique. The values estimated were of a smaller magnitude then one would expect of an airplane of this class. The wind tunnel estimate on the other hand predicted an unusual decrease in $C'_{m_q}$ with increasing angle of attack, which essentially implies an increase in short period damping. The comparison between flight and wind tunnel $C'_{m_q}$ s was therefore poor. The elevator effectiveness ($C'_{m_{\delta_e}}$) was lower than what wind tunnel predicted. A study of the spin parachute recovery system as a possible explanation gave no clue as to the cause of this discrepancy.

2. Lateral Parameters:

The β-derivatives were identifiable (standard errors less than 5 percent) and except for $C_{\ell_\beta}$ agreed with the wind-tunnel results (figure 18). $C_{\ell_\beta}$ was consistent until about 8° angle of attack and then there was an under-estimation of the parameter magnitude from there onwards. This could be due to the flow separation over the wing planform, resulting in a sluggish dihedral effect.

The p-derivatives with an exception of $C_{Y_p}$ were consistent with the wind-tunnel results for the entire angle of attack range (figure 19), the standard errors were under 7 percent. $C_{Y_p}$ is a less significant parameter since the airplane motion is not very sensitive to it, therefore, the lack of consistency is not considered critical.

The r-derivatives were generally consistent at low angles of attack, as shown in figure 20. Standard errors of the estimates were sometimes as high as 20 percent. The disagreement at higher angles of attack could be due to the spin recovery parachute canister which protrudes about 1/2 meter aft of the elevator trailing edge.

The effect of the aileron was easily determinable and errors of estimation were very small (less than 5 percent). The aileron effectiveness ($C_{\ell_{\delta_a}}$) agreed with the wind tunnel as shown in figure 21.

The effect of the rudder also agreed with the wind-tunnel results, standard errors of the estimates were less than 5 percent. A sharp drop in the magnitude of $C_{n_{\delta_r}}$ is apparent around 12° angle of attack (figure 22). This could be due to the effect of the wing wake on the vertical fin. At higher angles of attack the vertical fin is below the wake resulting in an improvement in the rudder effectiveness.

An high angles of attack the SR technique yielded numerous nonlinear terms (Appendix A), which have not been discussed. The discrepancies in flight and wind tunnel determined parameters in such regimes can be attributed to the effect that has been absorbed in such terms.

The ultimate test for the validity of the model was a comparison between the measured and simulated response of an airplane when subjected to the same input. The simulated data were generated using the parameters estimated from the SR algorithm. Models estimated at different flight conditions were tested and in most cases the prediction capability was good. Typical comparisons for the longitudinal and lateral maneuvers are given in figures 23 and 24.

## CONCLUDING REMARKS

A complete set of stability and control parameters for a general aviation aircraft was obtained from flight data. The standard errors of the main derivatives varied between 1 and 10 percent, errors were higher for parameters of lesser importance. Most of these parameters agreed with the wind tunnel estimates. Additional work is required to explain the discrepancies observed in the longitudinal rotary derivatives. Based on the estimates the airplane response was predicted well for the 4 to 20 degrees angle of attack range.

## REFERENCES

1. Gerlach, O. H.: Determination of Performance Stability and Control Characteristics from Measurements in Nonsteady Maneuvers. Stability and Control - Part 1, AGARD CP No. 17, September 1966, pp. 499-523.

2. Howard, J.: The Determination of Lateral Stability and Control Derivatives from Flight Data. Can. Aeron. and Space J., Vol. 13, No. 3, March 1967, pp. 127-134.

3. Suit, William T.: Aerodynamic Parameters of the Navion Airplane Extracted from Flight Data. NASA TN D-6643, 1972.

4. Cannaday, Robert L.; and Suit, William T.: Effect of Control Inputs on the Estimation of Stability and Control Parameters of a Light Airplane. NASA TP-1043, 1977.

5. Park, G. D.: Determination of Tail-Off Aircraft Parameters Using Systems Identification. Proceeding of the Third AIAA Atmospheric Flight Mechanics Conference, June 1976, pp. 128-136.

6. Queijo, M. J.; Wells, W. R.; and Keskar, D. A.: Approximate Indicial Lift Function for Tapered, Swept Wings in Incompressible Flow. NASA TP-1241, August 1978.

7. Queijo, M. J.; Wells, W. R.; and Keskar, D. A.: Inclusion of Unsteady Aerodynamics in Longitudinal Parameter Estimation from Flight Data. NASA TP-1536, December 1979.

8. Klein, V.: Maximum Likelihood Method for Estimating Airplane Stability and Control Parameters from Flight Data in Frequency Domain. NASA TP-1237, May 1980.

9. Wells, W. R.; Bonda, S. S.; and Quam, D. L.: Aircraft Lateral Parameter Estimation from Flight Data with Unsteady Aerodynamic Modeling. AIAA Paper 81-0221, 19th Aerospace Sciences Meeting, January 1981.

10. Klein, V.: Determination of Stability and Control Parameters of a Light Airplane from Flight Data Using Two Estimation Methods. NASA TP-1306, 1979.

11. Klein, V.; and Batterson, J. G.: Determination of Airplane Aerodynamic Parameters from Flight Data at High Angles of Attack. ICAS paper 82-6.3.3, August 1982.

12. Klein, V.; and Schiess, J. R.: Compatibility Check of Measured Aircraft Responses Using Kinematic Equations and Extended Kalman Filter. NASA TN-8514, 1977.

13. Klein, V.: Identification Evaluation Methods. Parameter Identification, AGARD-LS-104, 1979; pp. 2-1 through 2-21.

14. Klein, V.; Batterson, J. G.; and Murphy, P. C.: Determination of Airplane Model Structure from Flight Data by Using Modified Stepwise Regression. NASA TP-1916, October 1981.

15. Draper, N. R.; and Smith, H.: Applied Regression Analysis. John Wiley and Sons, Inc., c. 1966.

16. Taylor, L. W.; Iliff, K. W.: Systems Identification Using a Modified Newton-Raphson Method - A FORTRAN Program. NASA TN D-6734, 1972.

17. Grove, Randall D.; Bowles, Roland L.; and Mayhew, Stanley C.: A Procedure for Estimating Stability and Control Parameters from Flight Test Data by Using Maximum Likelihood Methods Employing a Real-Time Digital System. NASA TN D-6735, 1972.

18. Batterson, J. G.: Estimation of Airplane Stability and Control Derivatives from Large Amplitude Longitudinal Maneuvers. NASA TM-83185, October 1981.

19. Newson, W. A.; Satran, D. R.; and Johnson, J. L.: Effect of Wing-Leading Edge Modification on a Full-Scale, Low-Wing General Aviation Airplane - Wind Tunnel Investigation of High-Angle-of-Attack Aerodynamic Characteristics. NASA TP-2011, June 1982.

20. Cline, A. K.: Smoothing by Splines Under Tension. Department of Computer Sciences and Center for Numerical Analysis. University of Texas at Austin. CNA-168, 1981.

## APPENDIX A

### Equations of Motion

The airplane equations of motion are referred to the body axes (see figure 25). These equations are based on the following assumptions:

1. the airplane is a rigid body,
2. the effect of spinning rotors are negligible,
3. the airplane has a plane of symmetry XZ,
4. the airplane motion from initial reference conditions consists of small perturbations.

Based on the above assumptions, the equations of motion are expressed as:

$$\dot{u} = -qw + rv - g\sin\theta + \frac{\rho V^2 S}{2m} C_X \tag{A1}$$

$$\dot{v} = -ru + pw + g\cos\theta\sin\phi + \frac{\rho V^2 S}{2m} C_Y \tag{A2}$$

$$\dot{w} = -pv + qu + g\cos\theta\cos\phi + \frac{\rho V^2 S}{2m} C_Z \tag{A3}$$

$$\dot{p} = qr\left(\frac{I_Y - I_Z}{I_X}\right) + \frac{I_{XZ}}{I_X}(pq + \dot{r}) + \frac{\rho V^2 Sb}{2I_X} C_\ell \tag{A4}$$

$$\dot{q} = pr\left(\frac{I_Z - I_X}{I_Y}\right) + \frac{I_{XZ}}{I_Y}(r^2 - p^2) + \frac{\rho V^2 S\bar{c}}{2I_Y} C_m \tag{A5}$$

$$\dot{r} = pq\left(\frac{I_X - I_Y}{I_Z}\right) + \frac{I_{XZ}}{I_Z}(\dot{p} - qr) + \frac{\rho V^2 Sb}{2I_Z} C_n \tag{A6}$$

$$\dot{\theta} = q\cos\phi - r\sin\phi \tag{A7}$$

$$\dot{\phi} = p + (q\sin\phi + r\cos\phi)\tan\theta \tag{A8}$$

where

$$C_X = C_T\cos\varepsilon + C_L\sin\alpha - C_D\cos\alpha \tag{A9}$$

$$C_Z = C_T\sin\varepsilon + C_L\cos\alpha - C_D\sin\alpha \tag{A10}$$

For the equation error method, the aerodynamic coefficients were calculated from the measured quantities as follows:

$$C_X = \frac{mg}{\bar{q}S} a_X \tag{A11}$$

$$C_Y = \frac{mg}{\bar{q}S} a_Y \tag{A12}$$

$$C_Z = \frac{mg}{\bar{q}S} a_Z \tag{A13}$$

$$C_\ell = \frac{I_X}{\bar{q}Sb}\left[\dot{p} - \left(\frac{I_Y - I_Z}{I_X}\right) qr - \frac{I_{XZ}}{I_X} (pq + \dot{r})\right] \tag{A14}$$

$$C_m = \frac{I_Y}{\bar{q}S\bar{c}}\left[\dot{q} - \left(\frac{I_Z - I_X}{I_Y}\right) pr - \frac{I_{XZ}}{I_Y} (r^2 - p^2)\right] \tag{A15}$$

$$C_n = \frac{I_Z}{\bar{q}Sb}\left[\dot{r} - \left(\frac{I_X - I_Y}{I_Z}\right) pq - \frac{I_{XZ}}{I_Z} (\dot{p} - qr)\right] \tag{A16}$$

The aerodynamic coefficients were postulated as functions of the state and input variables and their combinations:

(a) The longitudinal coefficients $C_X$, $C_Z$, and $C_m$ as functions of $\alpha$, $q$, $\delta_e$, $\alpha^2$ $\alpha q$, $\alpha\delta_e$, $\beta^2$, $\alpha\beta^2$, $\alpha^3$, $\alpha^4$, $\alpha^5$, $\alpha^6$, $\alpha^7$, $\alpha^8$.

(b) The lateral coefficients $C_Y$, $C_\ell$, and $C_n$ as functions of $\beta$, $p$, $r$, $\delta_a$, $\delta_r$ $\alpha\beta$, $\alpha p$, $\alpha r$, $\alpha\delta_a$, $\alpha\delta_r$, $\alpha^2\beta$, $\alpha^2 p$, $\alpha^2 r$, $\alpha^2\delta_a$, $\alpha^2\delta_r$, $\beta^2$, $\beta^3$, $\beta^4$, $\beta^5$, $\beta^3\alpha^2$, $\beta^3\alpha$, $\alpha$, $\alpha^2$, $\alpha^3$.

All the above variables and their combinations are the increments with respect to their trim values. Typical linear models for the longitudinal and lateral aerodynamic coefficients are as follows:

$$C_Z = C_{Z_o} + C_{Z_\alpha}(\alpha - \alpha_o) + C_{Z_q}\frac{q\bar{c}}{2V} + C_{Z_{\delta_e}}(\delta_e - \delta_{e_o}) \tag{A17}$$

$$\begin{aligned} C_n = {} & C_{n_o} + C_{n_\beta}(\beta - \beta_o) + C_{n_p}\frac{pb}{2V} + C_{n_r}\frac{rb}{2V} \\ & + C_{n_{\delta_a}}(\delta_a - \delta_{a_o}) + C_{n_{\delta_r}}(\delta_r - \delta_{r_o}) \end{aligned} \tag{A18}$$

To avoid identification problems, the linear pitching moment coefficient is defined as:

$$C'_m = C'_{m_o} + C'_{m_\alpha}(\alpha - \alpha_o) + C'_{m_q}\frac{q\bar{c}}{2V} + C'_{m_{\delta_e}}(\delta_e - \delta_{e_o}) \tag{A19}$$

where

$$C'_{m_o} = C_{m_o} + C_{m_{\dot{\alpha}}}\left(\frac{\rho S\bar{c}}{4m} C_{Z_o} + \frac{g\bar{c}}{2V^2} \cos\theta_o\right) \tag{A20}$$

$$C'_{m_\alpha} = C_{m_\alpha} + \frac{\rho S\bar{c}}{4m} C_{m_{\dot{\alpha}}} C_{Z_\alpha} \tag{A21}$$

$$C'_{m_q} = C_{m_q} + C_{m_{\dot{\alpha}}} \left(1 + \frac{\rho S\bar{c}}{4m} C_{Z_q}\right) \tag{A22}$$

$$C'_{m_{\delta_e}} = C_{m_{\delta_e}} + \frac{\rho S\bar{c}}{4m} C_{m_{\dot{\alpha}}} C_{Z_{\delta_e}} \tag{A23}$$

# APPENDIX B

## Wind Tunnel Data

A static force investigation was conducted on a full-scale model of the test airplane (reference 19). Various wing and tail modifications were tested for determining their effect on high angles of attack aerodynamics. The investigation covered angles of attack ranging from -9 to 41 degrees at a Reynolds number of $2.5 \times 10^6$, based on the mean aerodynamic chord.

All longitudinal forces and moments were presented in the wind-axes system, whereas all the lateral-directional forces and moments were in the body-axes system. Therefore, all the longitudinal forces were transformed into the body axes as follows:

$$C_X = -C_D \cos\alpha + C_L \sin\alpha \tag{B1}$$

$$C_Z = -C_D \sin\alpha - C_L \cos\alpha \tag{B2}$$

The derivatives with respect to the angle of attack were determined by putting a second order spline through the data and calculating the slope at each point (reference 20).

Based on (B1) and (B2), the derivatives in the body axis system were calculated from the expressions,

$$C_{X_\alpha} = (C_L - C_{D_\alpha})\cos\alpha + (C_D + C_{L_\alpha})\sin\alpha \tag{B3}$$

$$C_{Z_\alpha} = -(C_{L_\alpha} + C_D)\cos\alpha + (C_L - C_{D_\alpha})\sin\alpha \tag{B4}$$

The derivatives with respect to the control deflection were determined based on the coefficient changes over the entire angle of attack range.

$$A_\delta\Big|_{\alpha_i} = \frac{\Delta A}{\Delta \delta}\Big|_{\alpha_i} \tag{B5}$$

where A is $C_X$, $C_Y$, $C_Z$, $C_\ell$, $C_m$, or $C_n$; and $\delta$ is $\delta_e$, $\delta_a$, or $\delta_r$.

Transformation equations for the control derivatives for $C_X$ and $C_Z$ follow from (B1) and (B2) as follows

$$C_{X_{\delta_e}} = -C_{D_{\delta_e}} \cos\alpha + C_{L_{\delta_e}} \sin\alpha \tag{B6}$$

$$C_{Z_{\delta_e}} = -(C_{D_{\delta_e}} \sin\alpha + C_{L_{\delta_e}} \cos\alpha) \tag{B7}$$

$C_{m_\alpha}$ was transformed to the airplane Center of Gravity by

$$C_{m_\alpha} = (C_{m_\alpha})_{WT} - C_{L_\alpha}(h_{WT} - h) \tag{B8}$$

The values for $C_{Y_\beta}$, $C_{\ell_\beta}$, and $C_{n_\beta}$ were read directly from reference 19.

The dynamic derivatives were derived from the unpublished wind-tunnel tests that were run on a one-third scale model. A power spectral density analysis for both longitudinal and lateral transient maneuvers was required to determine the dominating frequencies.

For the longitudinal case k was determined to range between 0.028 and 0.04 for angles of attack ranging between 4 and 24 degrees. A similar analysis on lateral transient maneuvers between angles of attack 6 and 26 degrees yielded a k value ranging between 0.15 and 0.24, the wind tunnel data however unlike the longitudinal case was insensitive to this variation.

The following derivatives given in an unpublished wind-tunnel test report are:

$$C'_{Y_p} = C_{Y_p} + C_{Y_{\dot\beta}} \sin\alpha \tag{B9}$$

$$C'_{n_p} = C_{n_p} + C_{n_{\dot\beta}} \sin\alpha \tag{B10}$$

$$C'_{\ell_p} = C_{\ell_p} + C_{\ell_{\dot\beta}} \sin\alpha \tag{B11}$$

$$C'_{m_q} = C_{m_q} + C_{m_{\dot\alpha}} \tag{B12}$$

$$C'_{X_q} = -(C_{A_q} + C_{A_{\dot\alpha}}) \tag{B13}$$

$$C'_{Z_q} = -(C_{N_q} + C_{N_{\dot\alpha}}) \tag{B14}$$

$$C'_{Y_r} = C_{Y_r} - C_{Y_{\dot\beta}} \cos\alpha \tag{B15}$$

$$C'_{n_r} = C_{n_r} - C_{n_{\dot\beta}} \cos\alpha \tag{B16}$$

$$C'_{\ell_r} = C_{\ell_r} - C_{\ell_{\dot\beta}} \cos\alpha \tag{B17}$$

TABLE I.- PHYSICAL CHARACTERISTICS OF TEST AIRPLANE

| | |
|---|---|
| Wing (Modified NACA $64_2$-415) | |
| Span, m | 7.45 |
| Area, $m^2$ | 9.21 |
| Mean aerodynamic chord, m | 1.23 |
| Aspect ratio | 6.10 |
| Dihedral, deg | 5.00 |
| Wing incidence, deg | 3.50 |
| Aileron (each) | |
| Span, m | 1.16 |
| Area, $m^2$ | 0.24 |
| Chord, m | 0.21 |
| Flap (each) | |
| Span, m | 1.15 |
| Area, $m^2$ | 0.25 |
| Chord, m | 0.21 |
| Horizontal tail (NACA $65_1$-012) | |
| Span, m | 2.34 |
| Area, $m^2$ | 1.96 |
| Mean aerodynamic chord, m | 0.84 |
| Incidence, deg | -3.00 |
| Elevator | |
| Span, m | 2.34 |
| Area, $m^2$ | 0.77 |
| Root chord, m | 0.34 |
| Tip chord, m | 0.21 |
| Vertical tail (NACA $65_1$-012) | |
| Span, m | 1.25 |
| Area, $m^2$ | 1.20 |
| Root chord, m | 1.09 |
| Tip chord, m | 0.51 |
| Rudder | |
| Span, m | 1.25 |
| Area, $m^2$ | 0.33 |
| Root chord, m | 0.34 |
| Tip chord, m | 0.21 |
| Propeller diameter, m | 1.80 |
| Propeller pitch, m | 1.17 |

TABLE II.- ESTIMATE AND STANDARD ERRORS OF PARAMETERS

Longitudinal

| Parameter | Value | Standard Error |
|---|---|---|
| $C_{X_o}$ | -0.0806 | |
| $C_{X_\alpha}$ | 0.396 | 0.0076 |
| $C_{X_q}$ | 1.19 | 0.263 |
| $C_{X_{\delta_e}}$ | -0.115 | 0.0109 |
| $C_{X_{\alpha^2}}$ | 1.74 | 0.116 |

| Parameter | Value | Standard Error |
|---|---|---|
| $C_{Z_o}$ | -0.0554 | |
| $C_{Z_\alpha}$ | -3.43 | 0.0117 |
| $C_{Z_q}$ | -6.07 | 0.406 |
| $C_{Z_{\delta_e}}$ | -0.214 | 0.0169 |
| $C_{Z_{\alpha^2}}$ | 2.4 | 0.178 |

| Parameter | Value | Standard Error |
|---|---|---|
| $C'_{m_o}$ | 0.00279 | |
| $C'_{m_\alpha}$ | -0.223 | 0.00367 |
| $C'_{m_q}$ | -6.21 | 0.127 |
| $C'_{m_{\delta_e}}$ | -0.607 | 0.00526 |

TABLE II.- ESTIMATE AND STANDARD ERRORS OF PARAMETERS (concl'd)

Lateral

| Parameter | Value | Standard Error |
|---|---|---|
| $C_{Y_o}$ | 0.024 | |
| $C_{Y_\beta}$ | -0.328 | 0.0042 |
| $C_{Y_p}$ | 0.519 | 0.0204 |
| $C_{Y_r}$ | -0.374 | 0.0505 |
| $C_{Y_{\delta_a}}$ | 0.181 | 0.00442 |
| $C_{Y_{\delta_r}}$ | 0.0593 | 0.0039 |

| Parameter | Value | Standard Error |
|---|---|---|
| $C_{\ell_o}$ | -0.00113 | |
| $C_{\ell_\beta}$ | -0.0827 | 0.00174 |
| $C_{\ell_p}$ | -0.382 | 0.00844 |
| $C_{\ell_r}$ | 0.214 | 0.0209 |
| $C_{\ell_{\delta_a}}$ | -0.108 | 0.00183 |
| $C_{\ell_{\delta_r}}$ | 0.0152 | 0.00162 |
| $C_{\ell_{\delta_{\alpha^2\beta}}}$ | 14.5 | 2.03 |

| Parameter | Value | Standard Error |
|---|---|---|
| $C_{n_o}$ | -0.000559 | |
| $C_{n_\beta}$ | 0.0506 | 0.000596 |
| $C_{n_p}$ | -0.0769 | 0.00289 |
| $C_{n_r}$ | -0.0878 | 0.00716 |
| $C_{n_{\delta_a}}$ | -0.000272 | 0.000676 |
| $C_{n_{\delta_r}}$ | -0.0505 | 0.000553 |

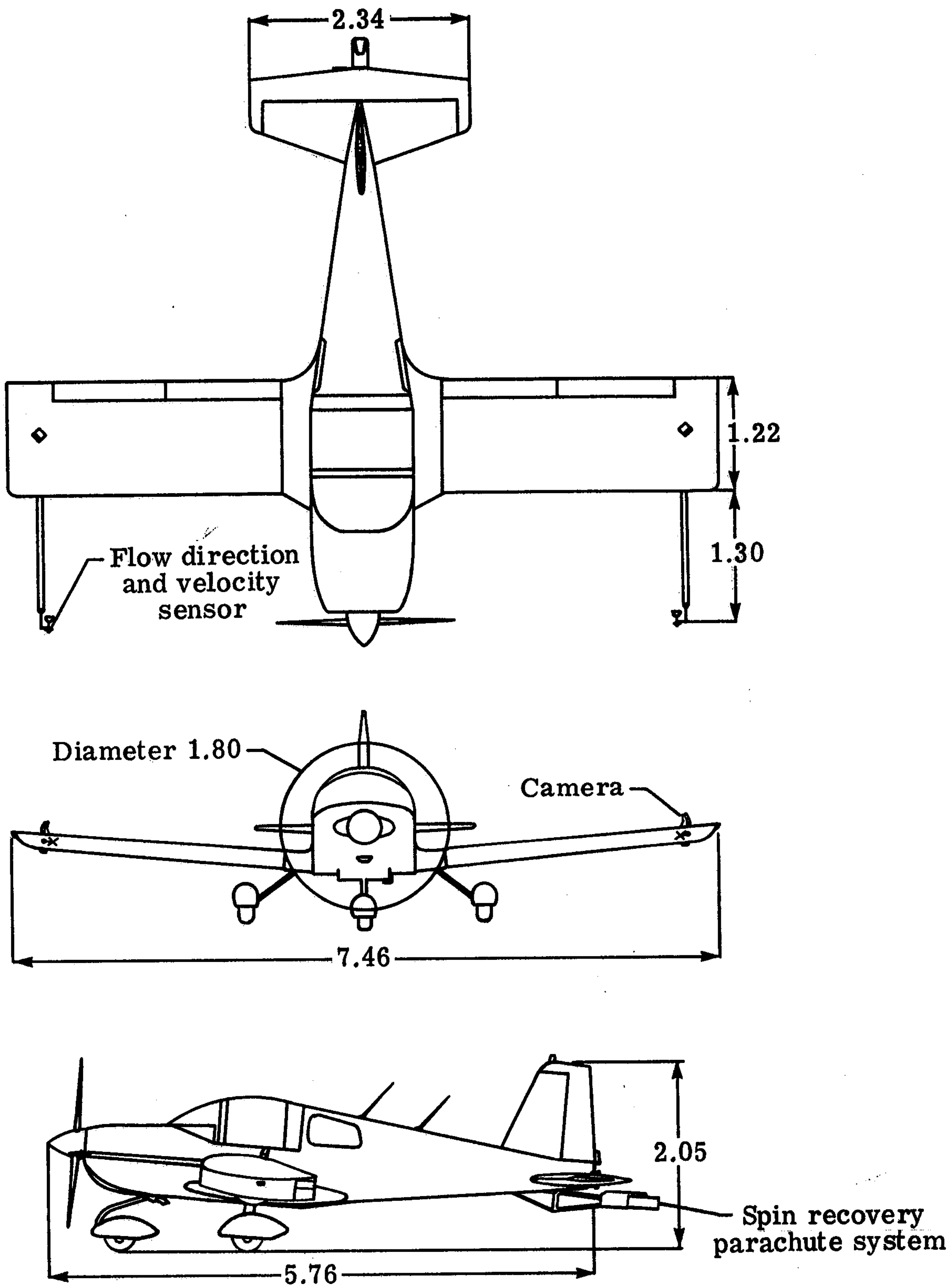


Figure 1.- Test airplane. Dimensions are in meters.

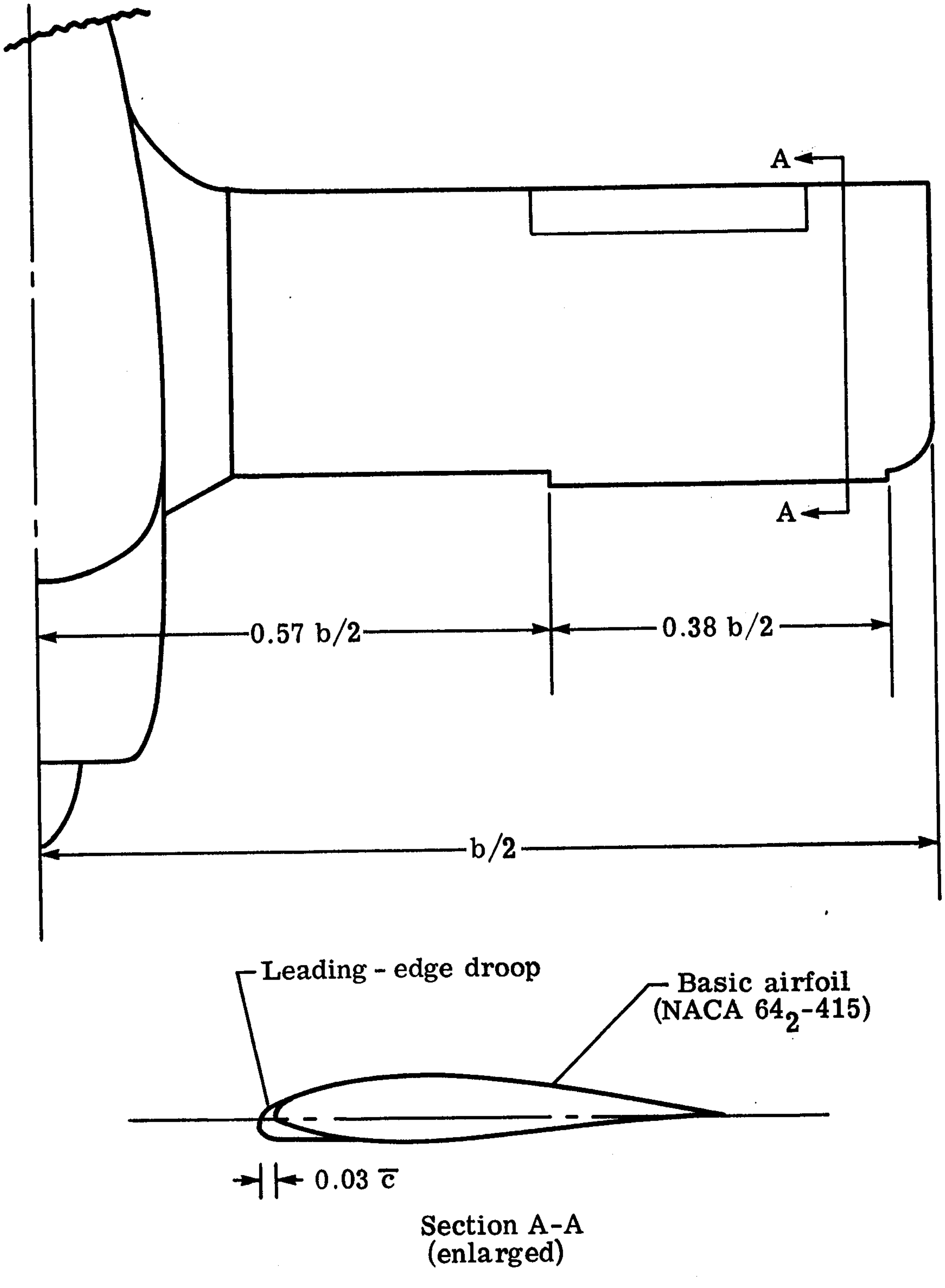


Figure 2.- Configuration with droop outboard leading edge.

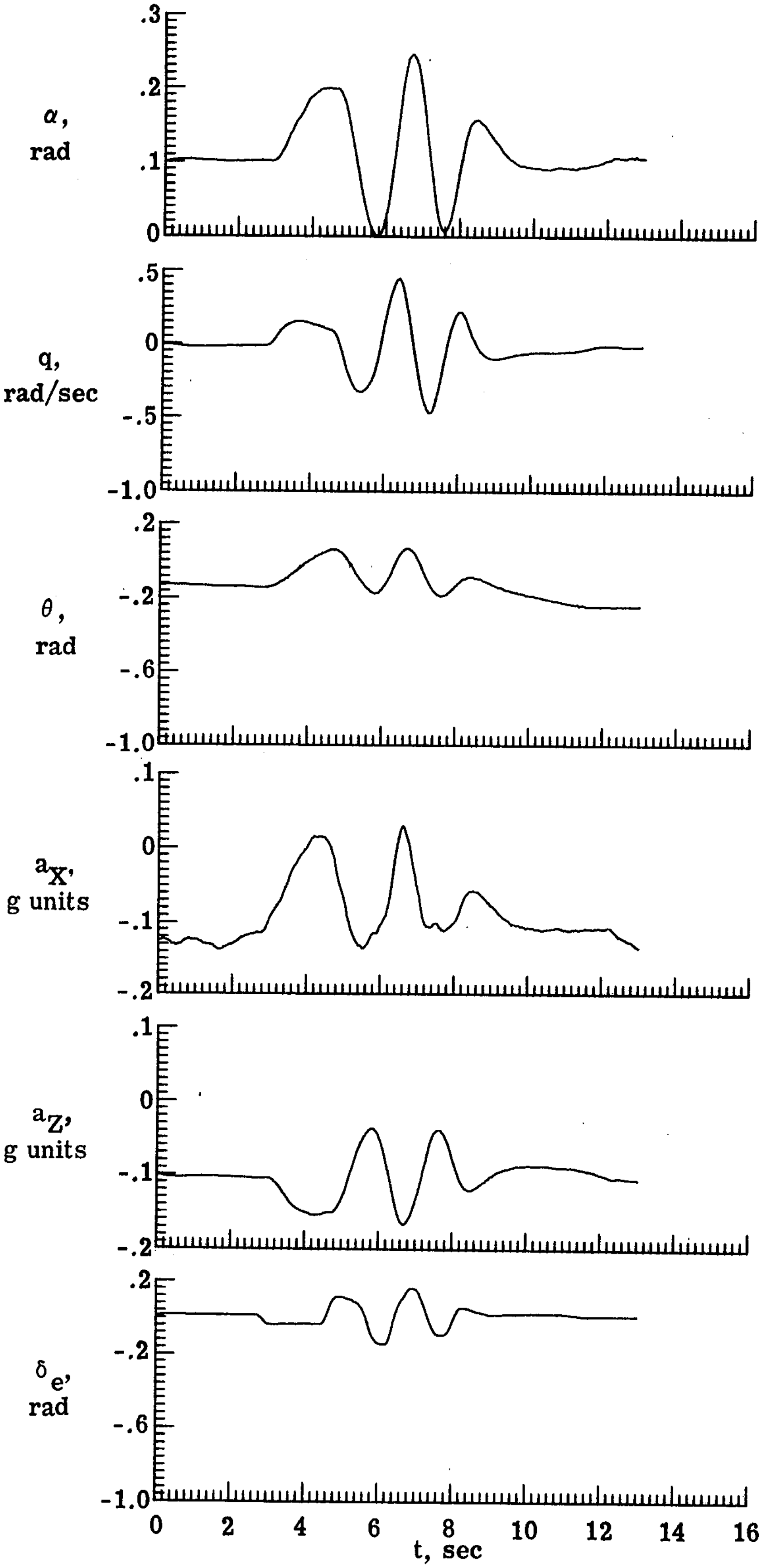


Figure 3.- Longitudinal transient maneuver.

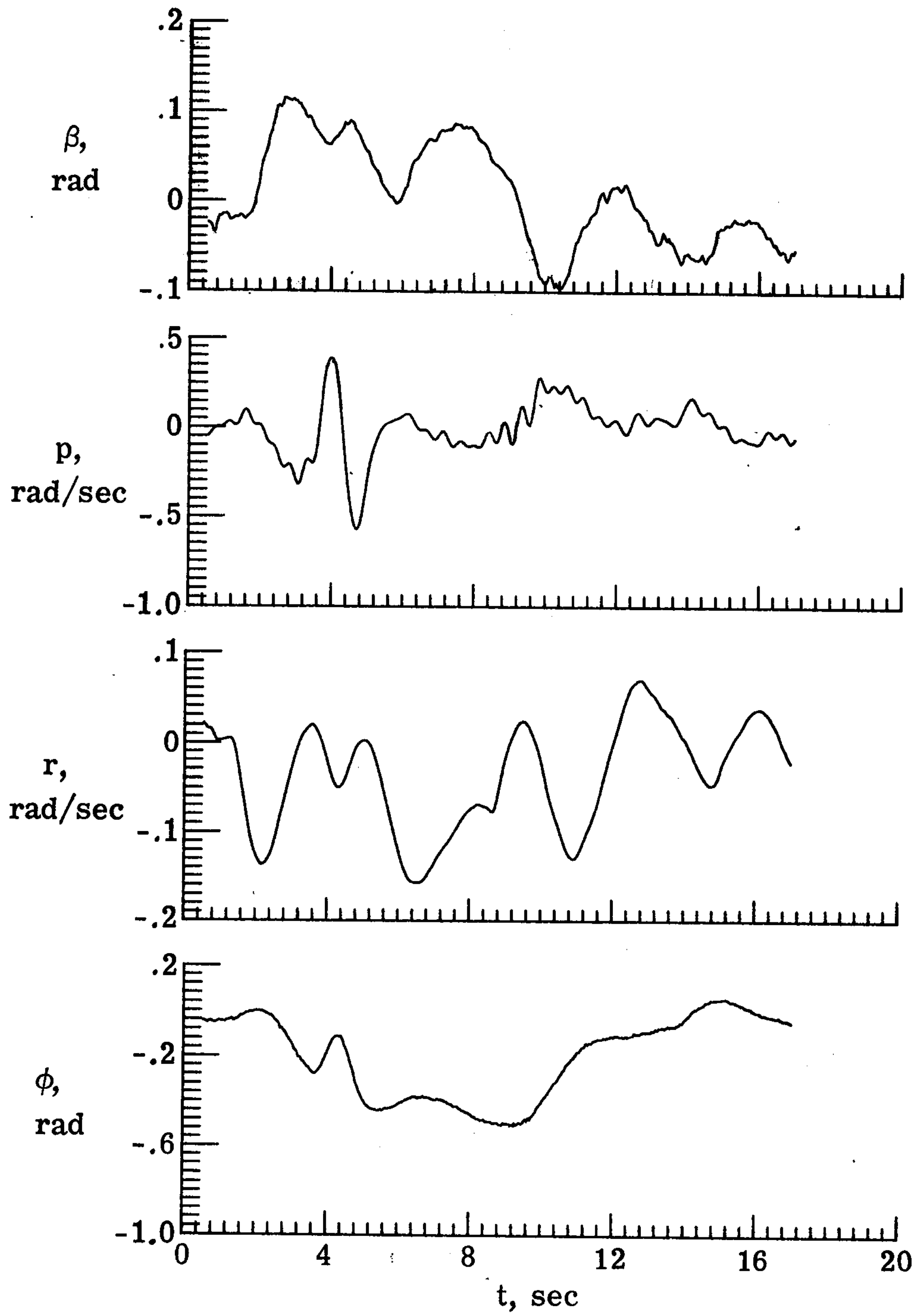


Figure 4.- Lateral transient maneuver.

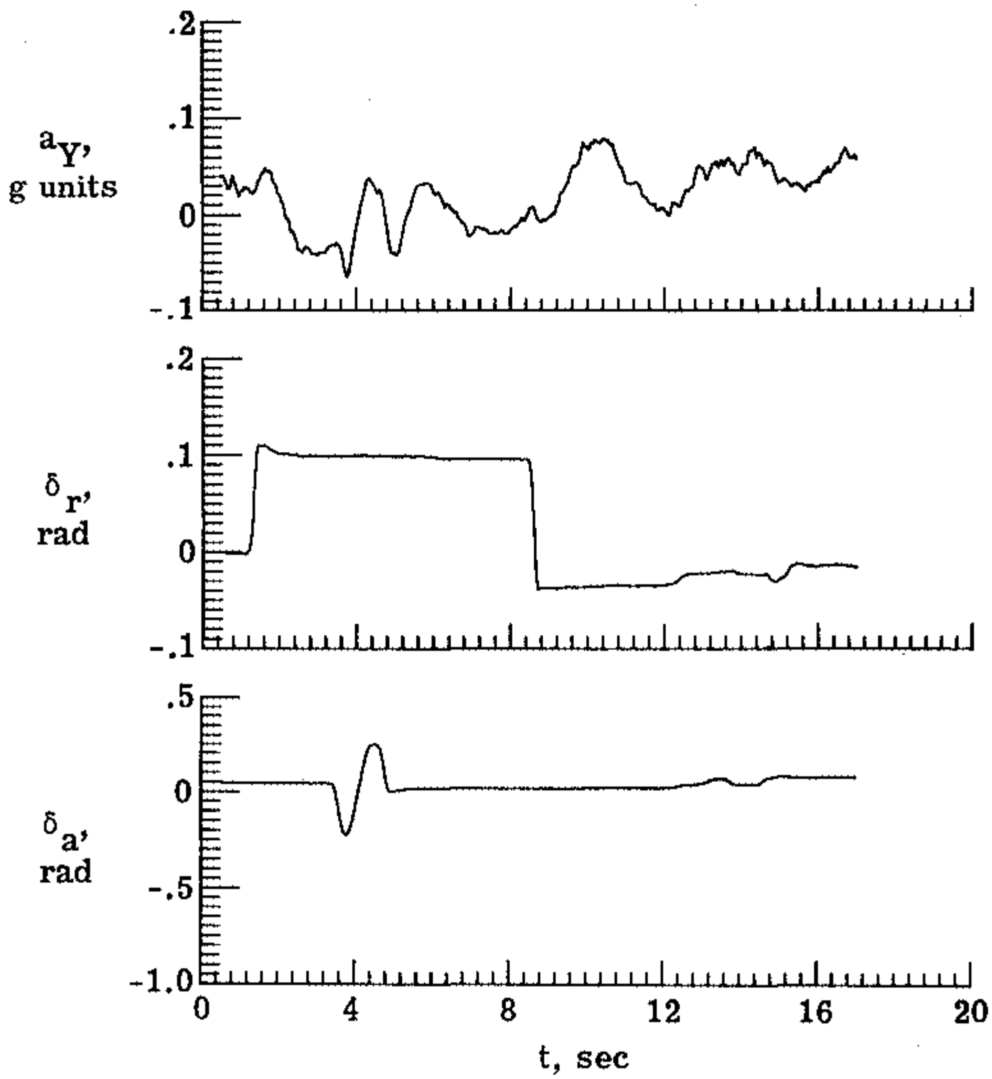


Figure 4.- Concluded.

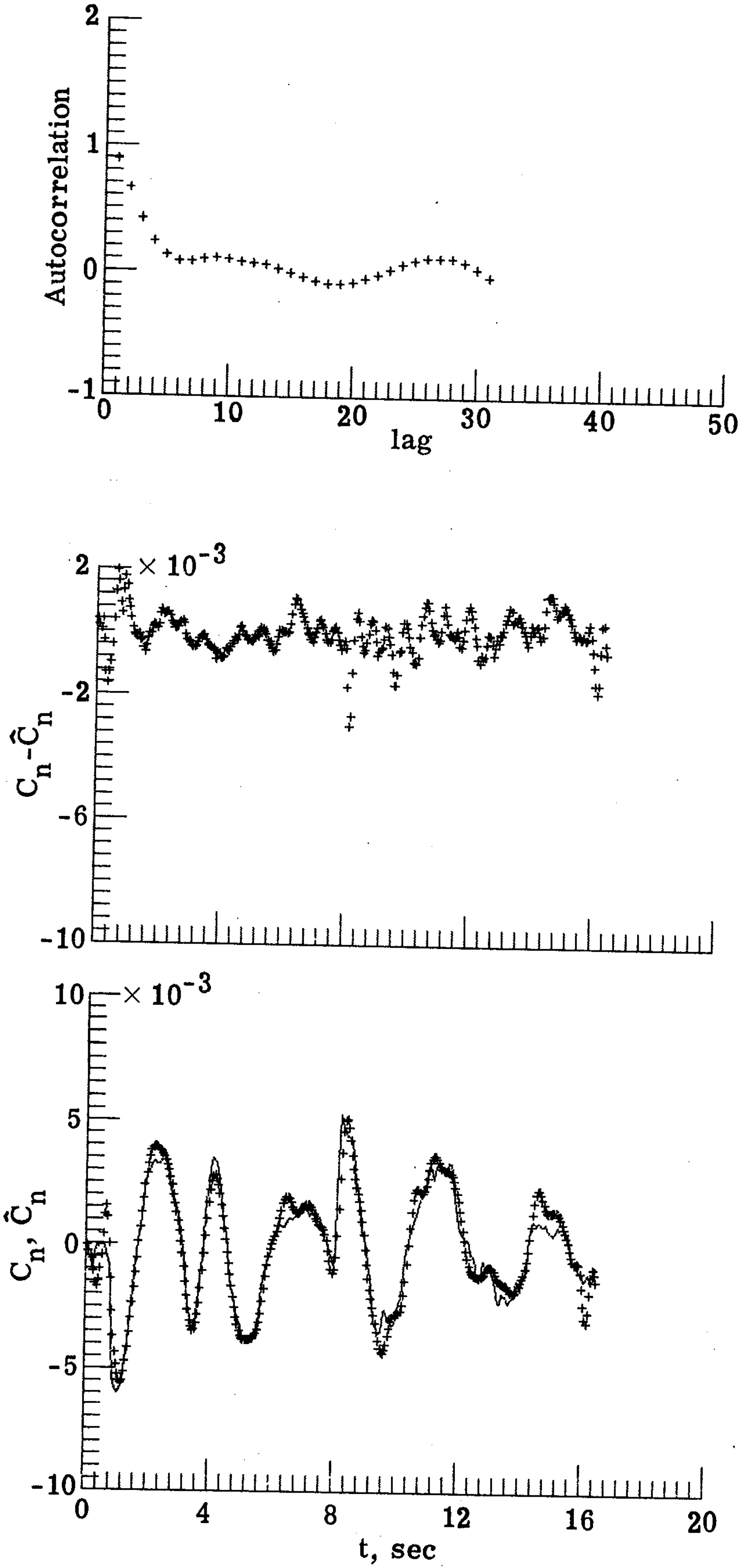


Figure 5.- Model characteristics from stepwise regression technique.

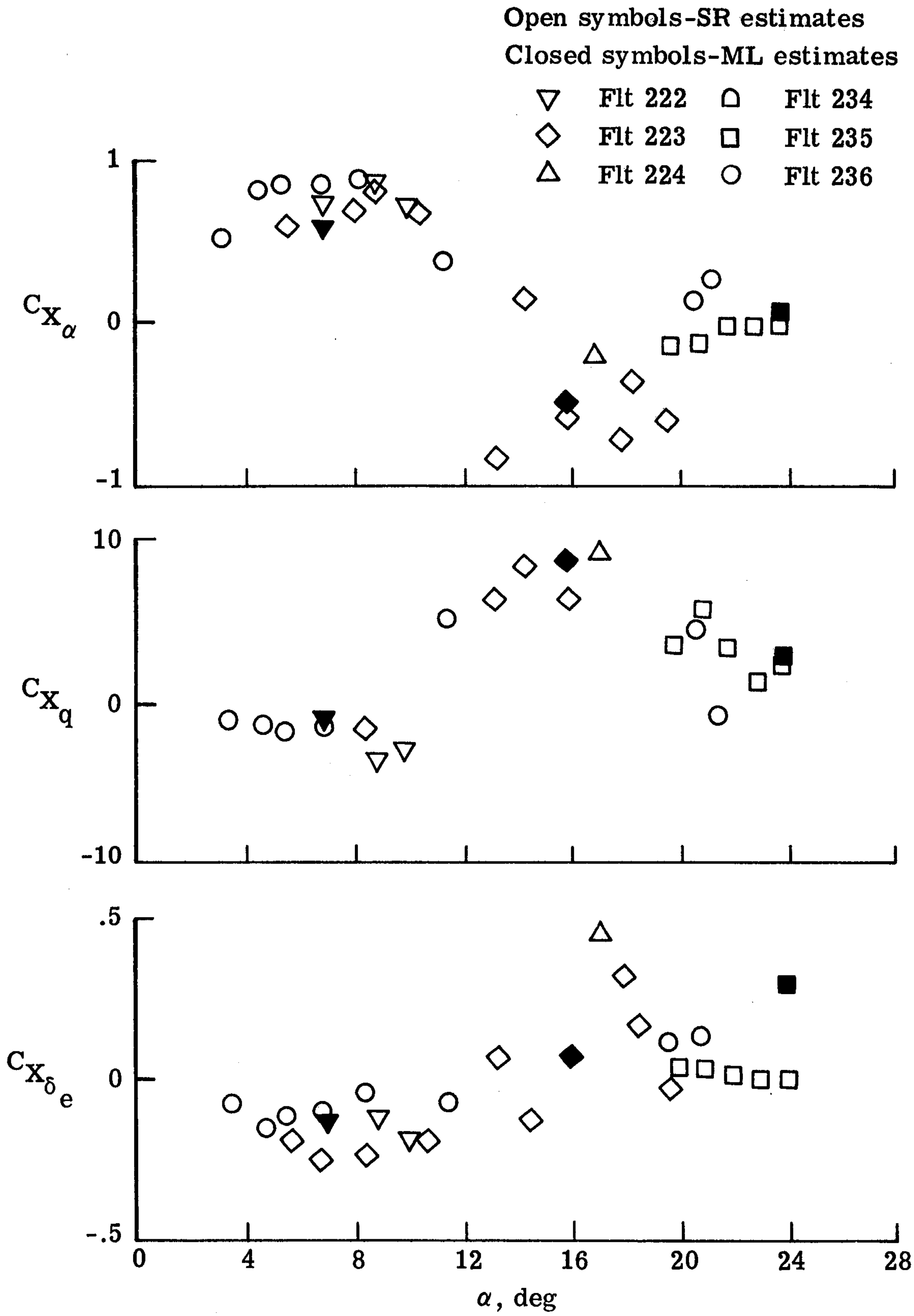


Figure 6.- Longitudinal-force derivatives estimated from flight data.

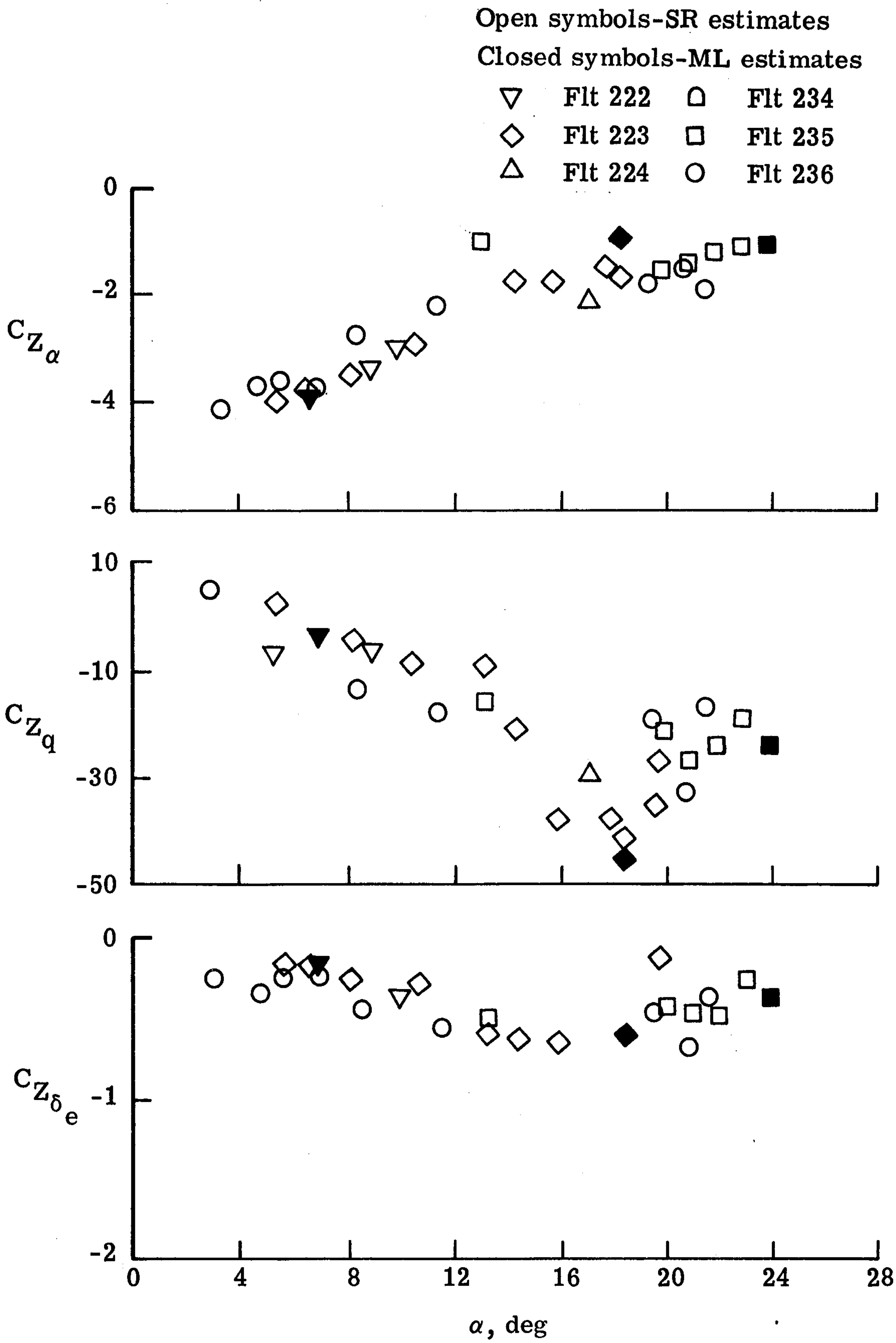


Figure 7.- Vertical-force derivatives estimated from flight data.

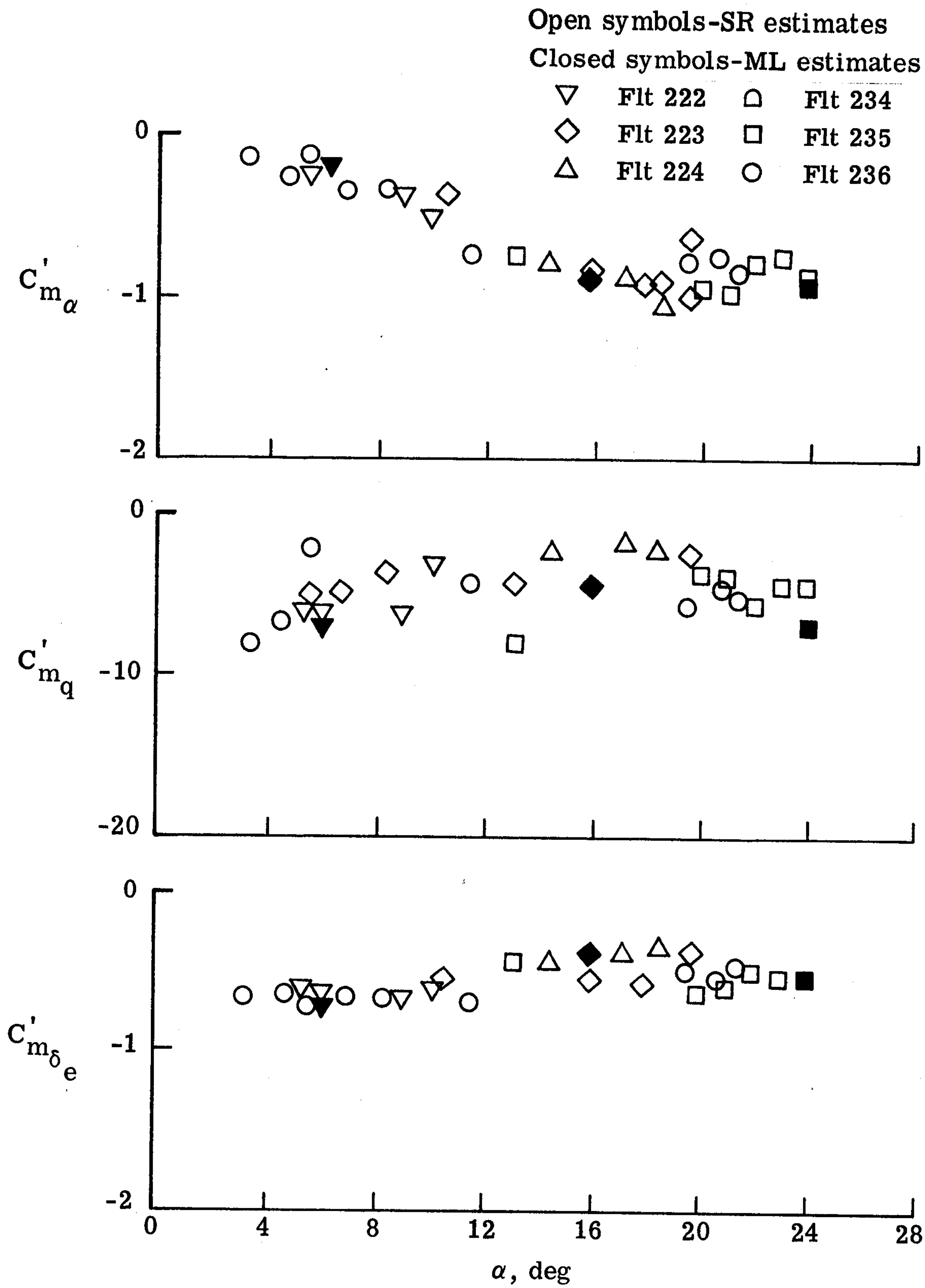


Figure 8.- Pitching-moment derivatives estimated from flight data.

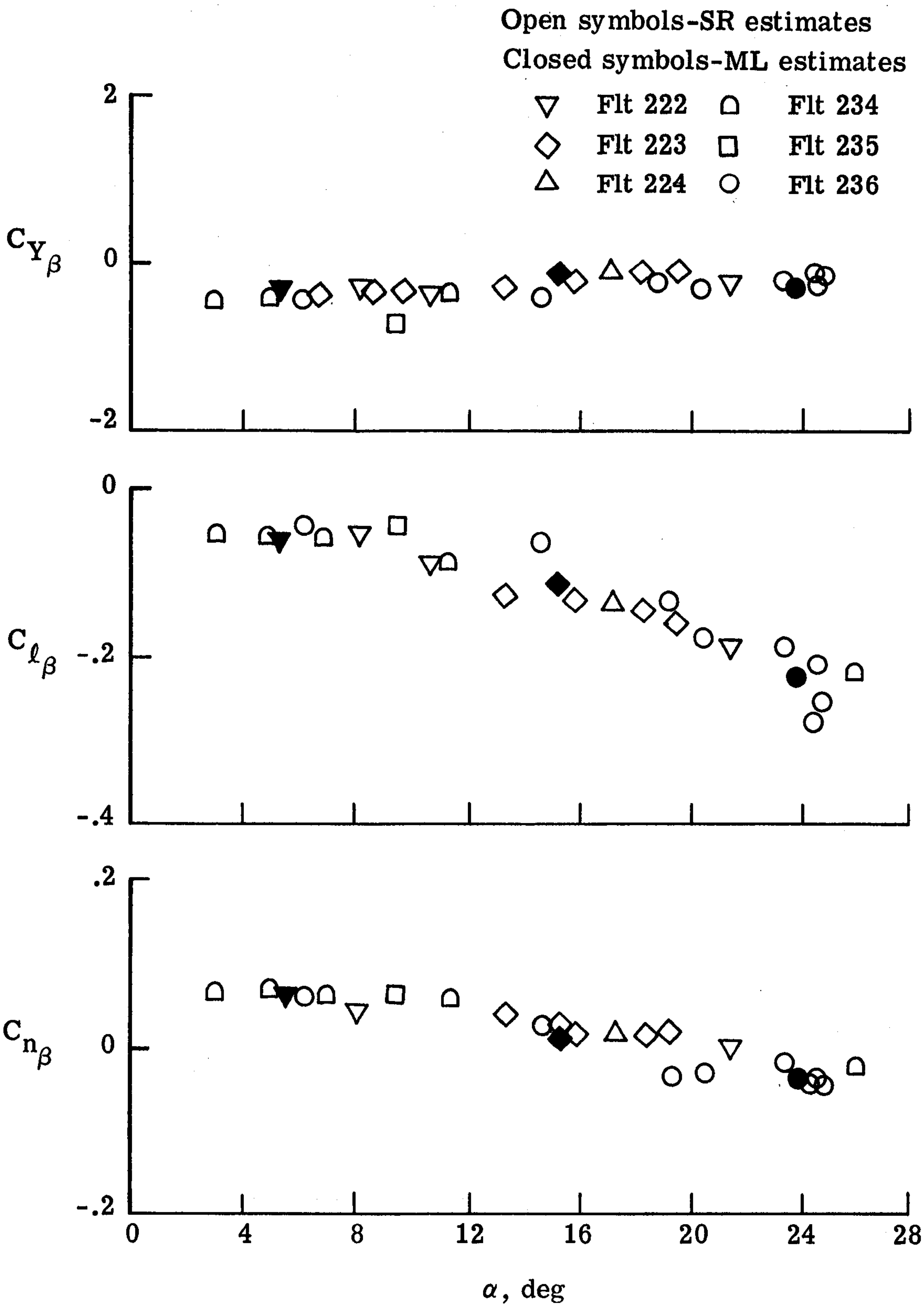


Figure 9.- Sideslip derivatives estimated from flight data.

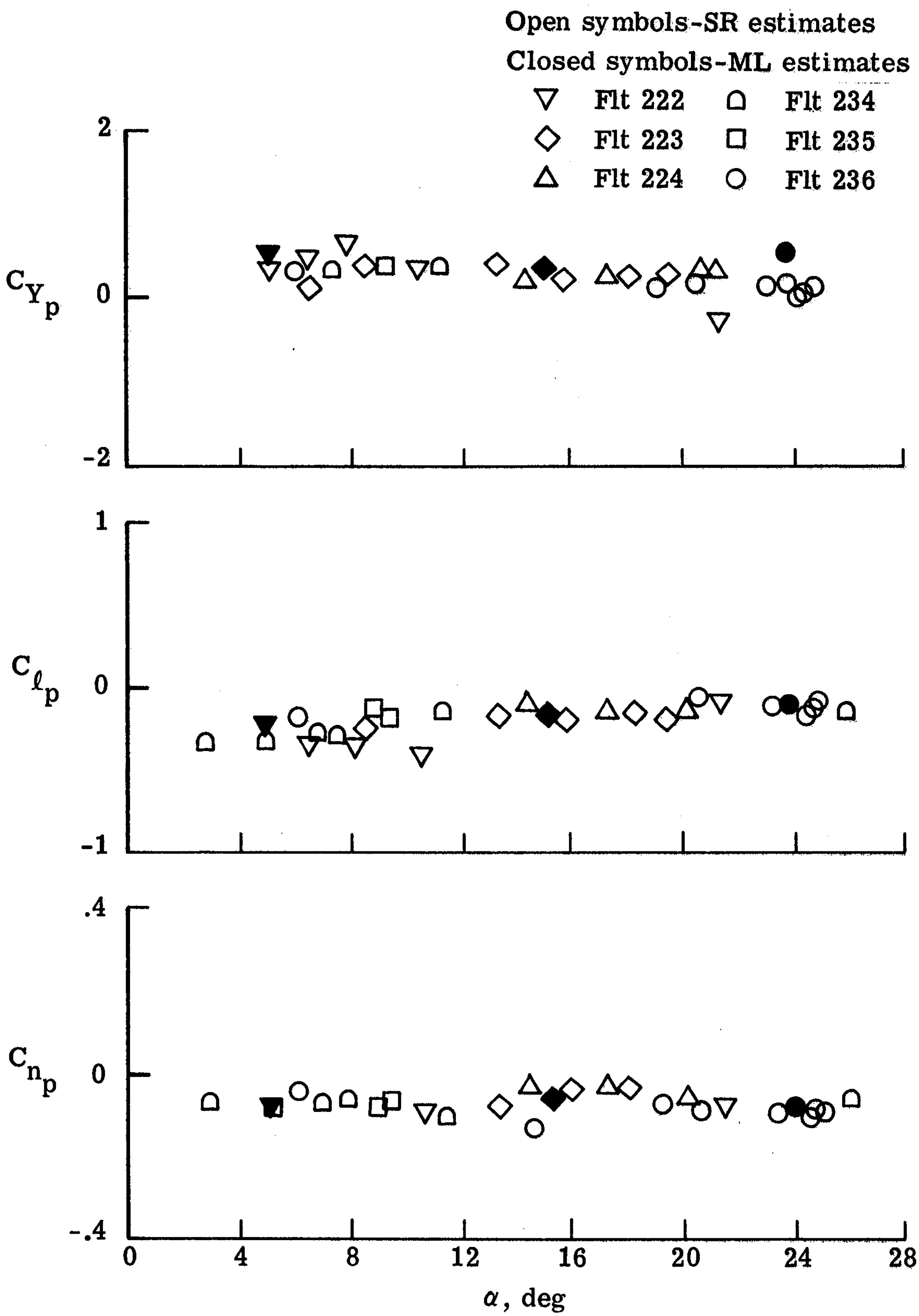


Figure 10.- Roll-rate derivatives estimated from flight data.

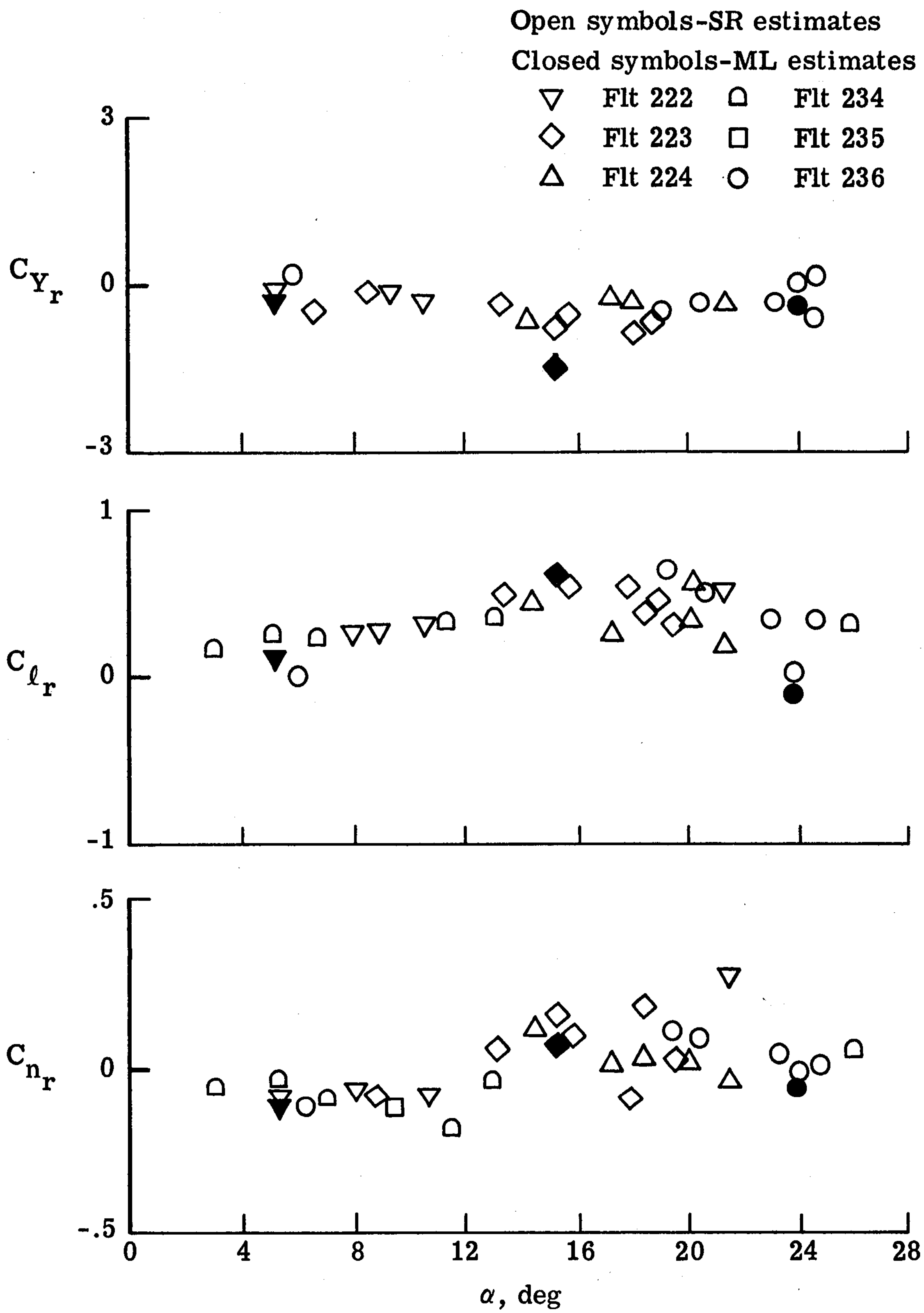


Figure 11.- Yaw-rate derivatives estimated from flight data.

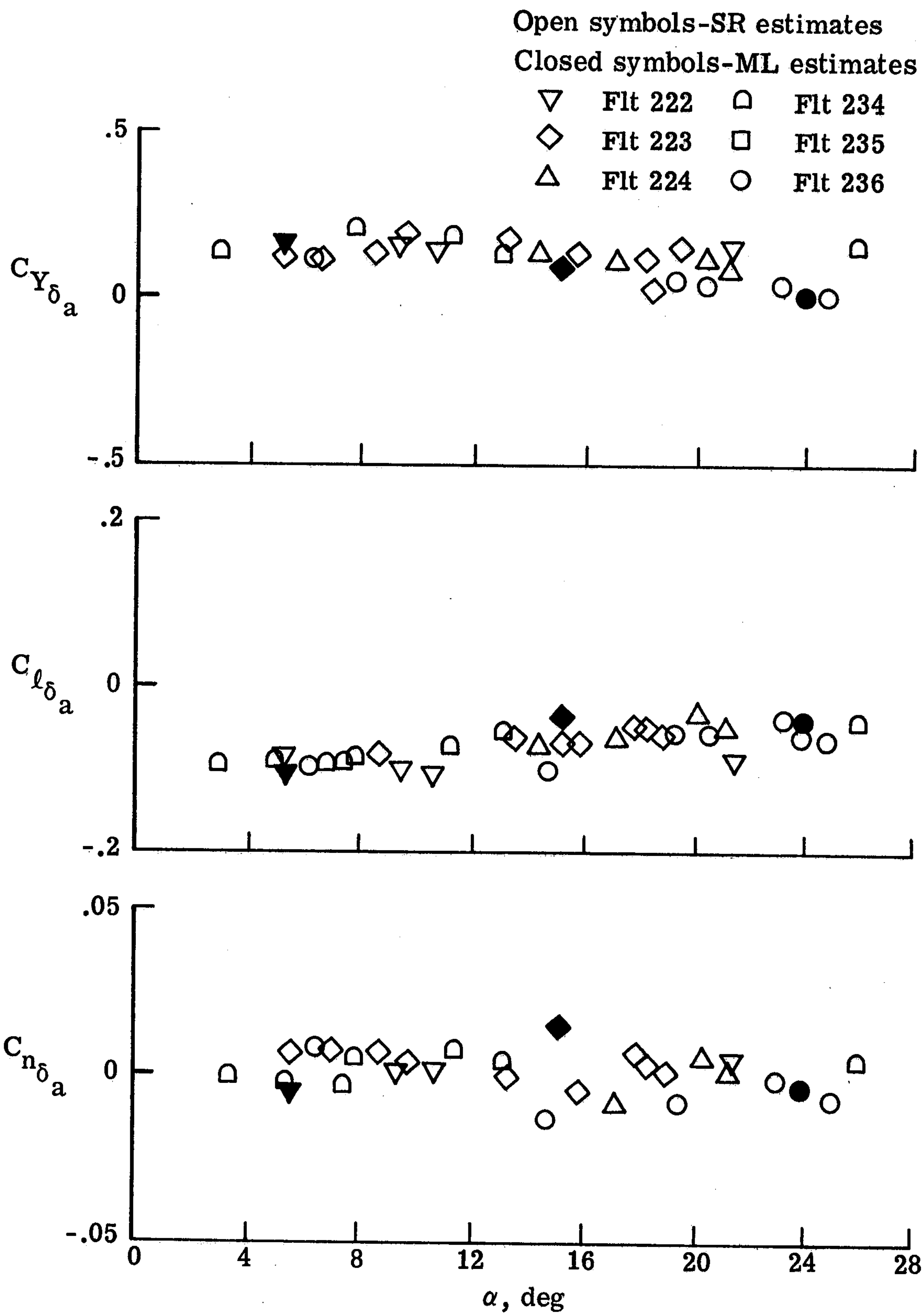


Figure 12.- Aileron derivatives estimated from flight data.

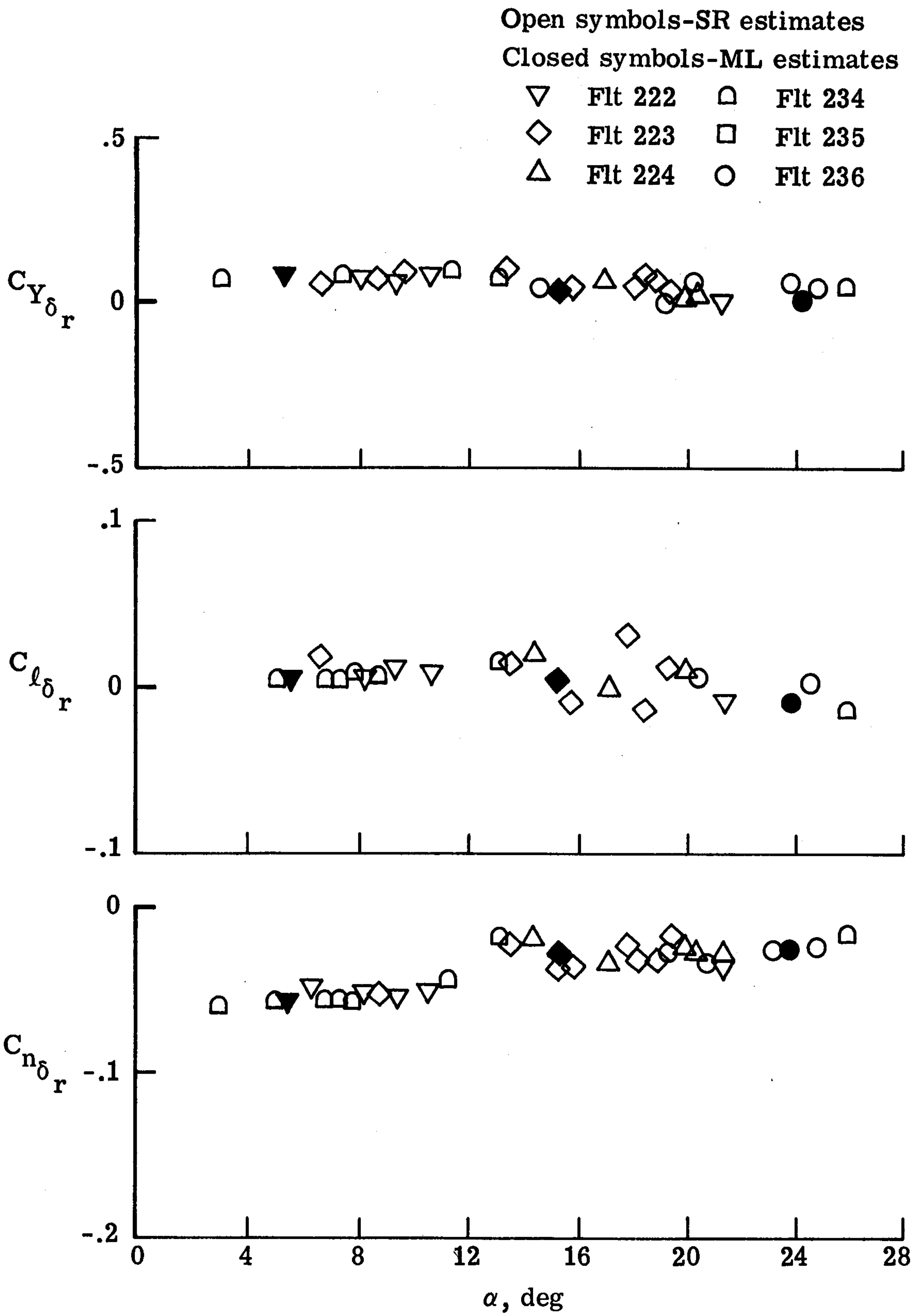


Figure 13.- Rudder derivatives estimated from flight data.

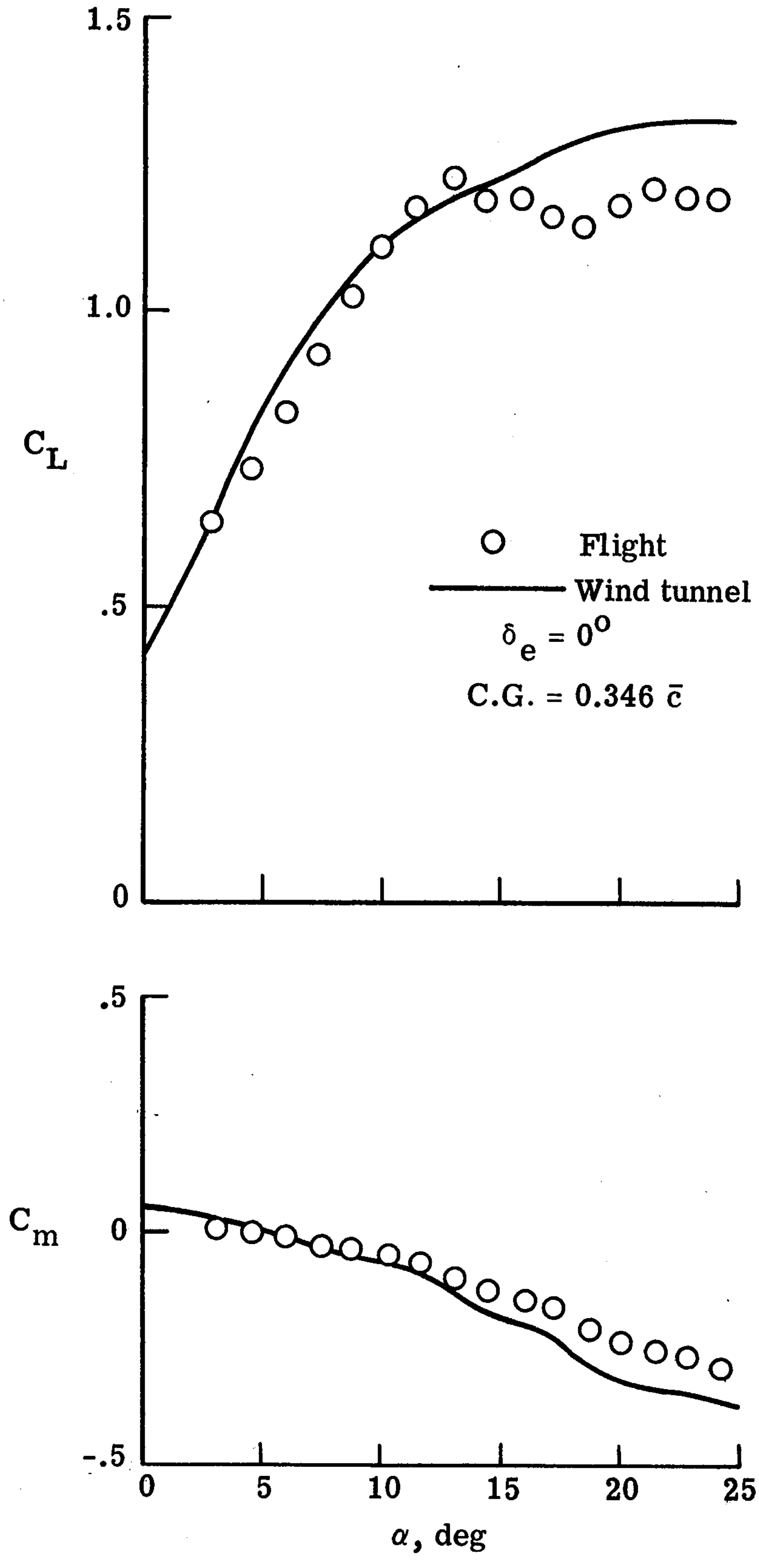


Figure 14.- Lift and pitching-moment coefficients determined from flight and wind tunnel data.

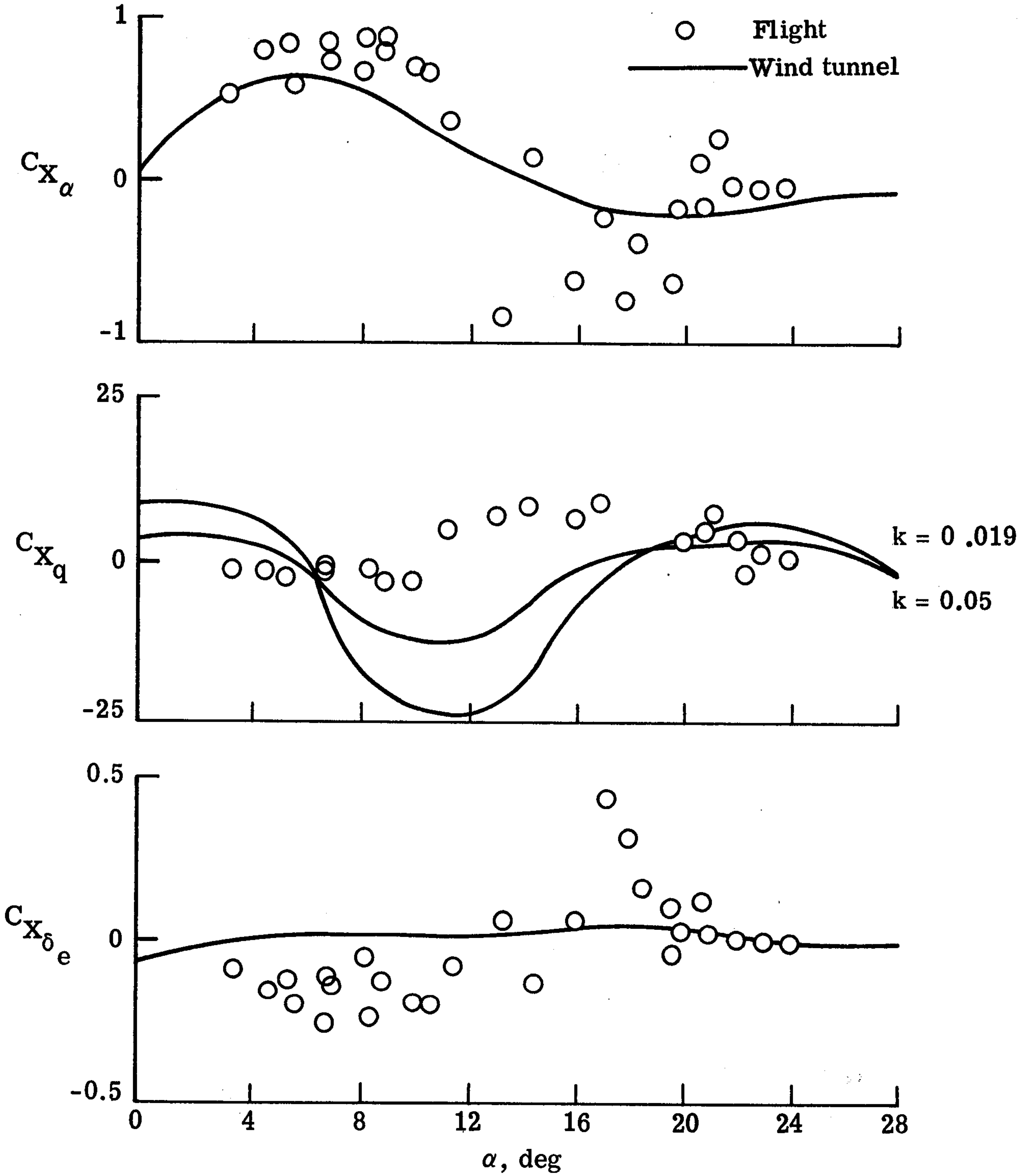


Figure 15.- Comparison of longitudinal-force derivatives determined from flight and wind tunnel.

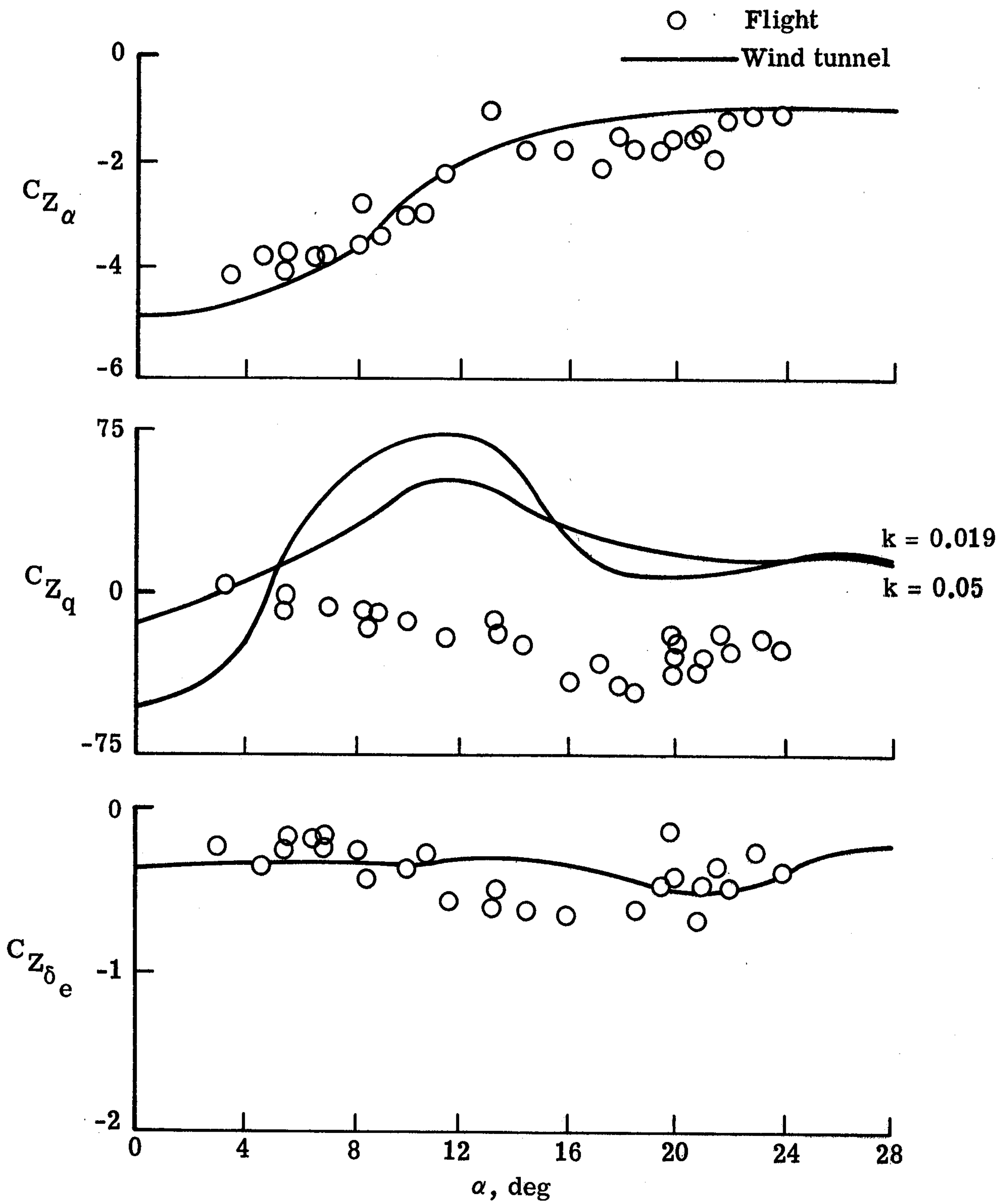


Figure 16.- Comparison of vertical-force derivatives determined from flight and wind tunnel.

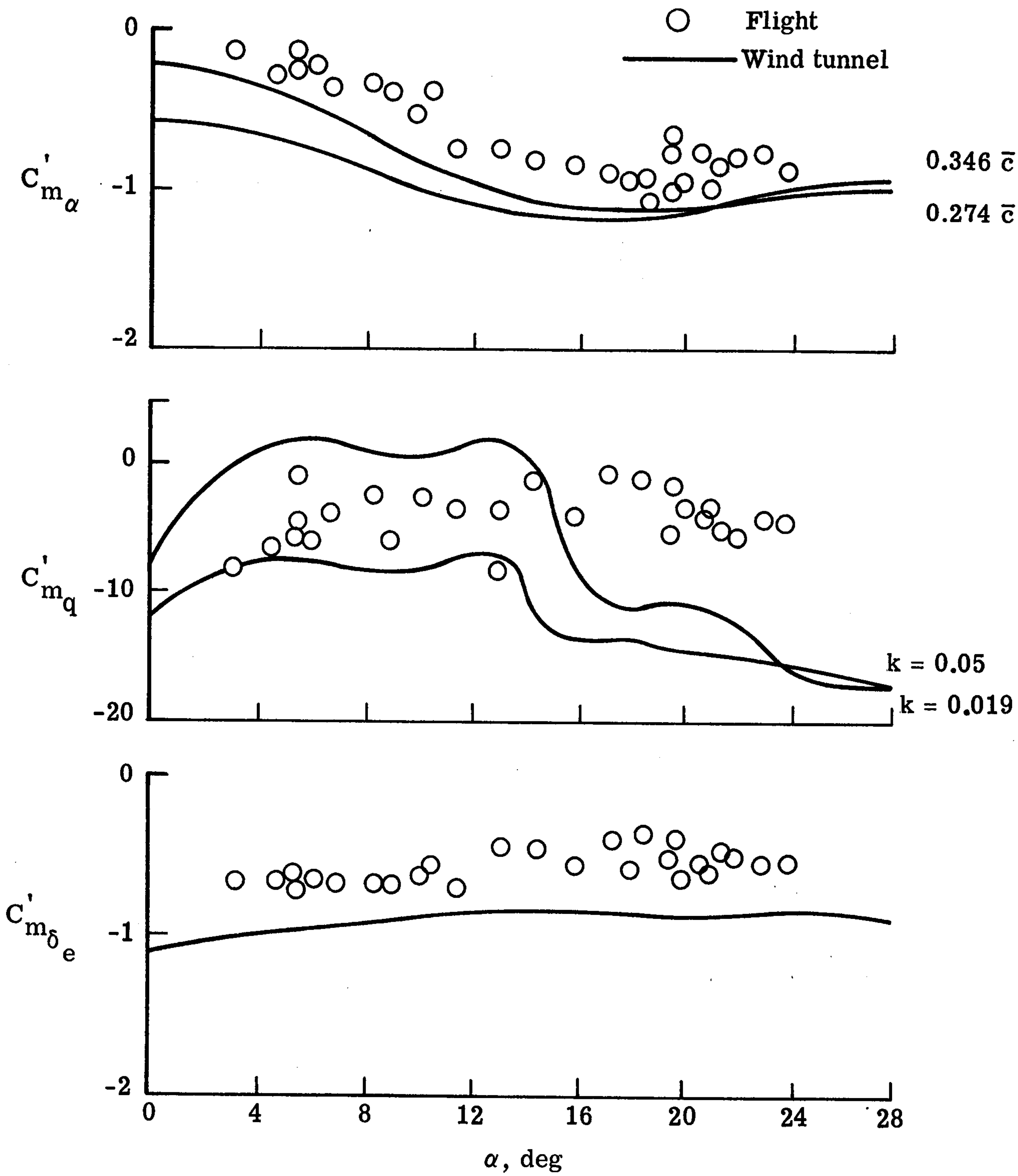


Figure 17.- Comparison of pitching-moment derivatives determined from flight and wind tunnel.

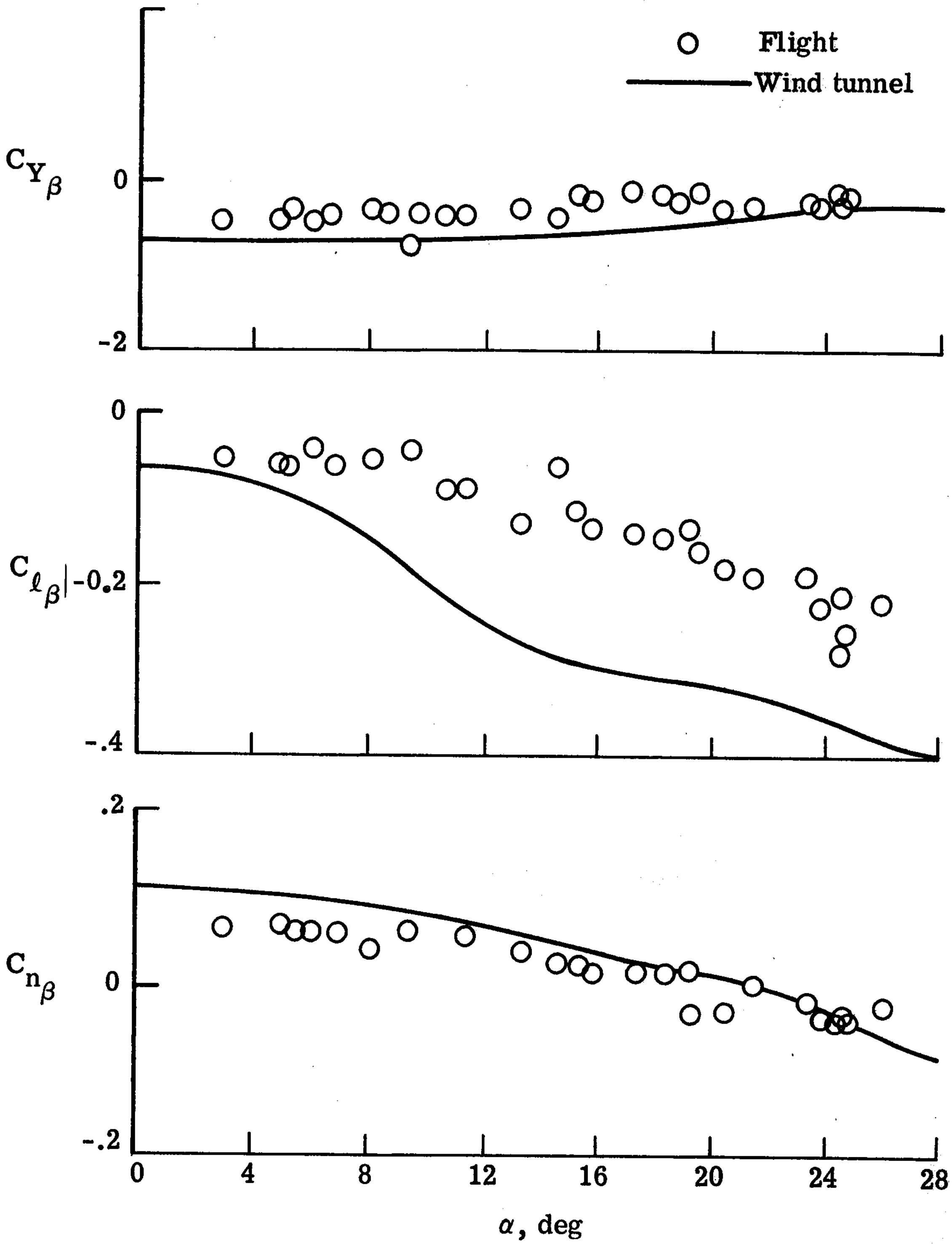


Figure 18.- Comparison of sideslip derivatives determined from flight and wind tunnel.

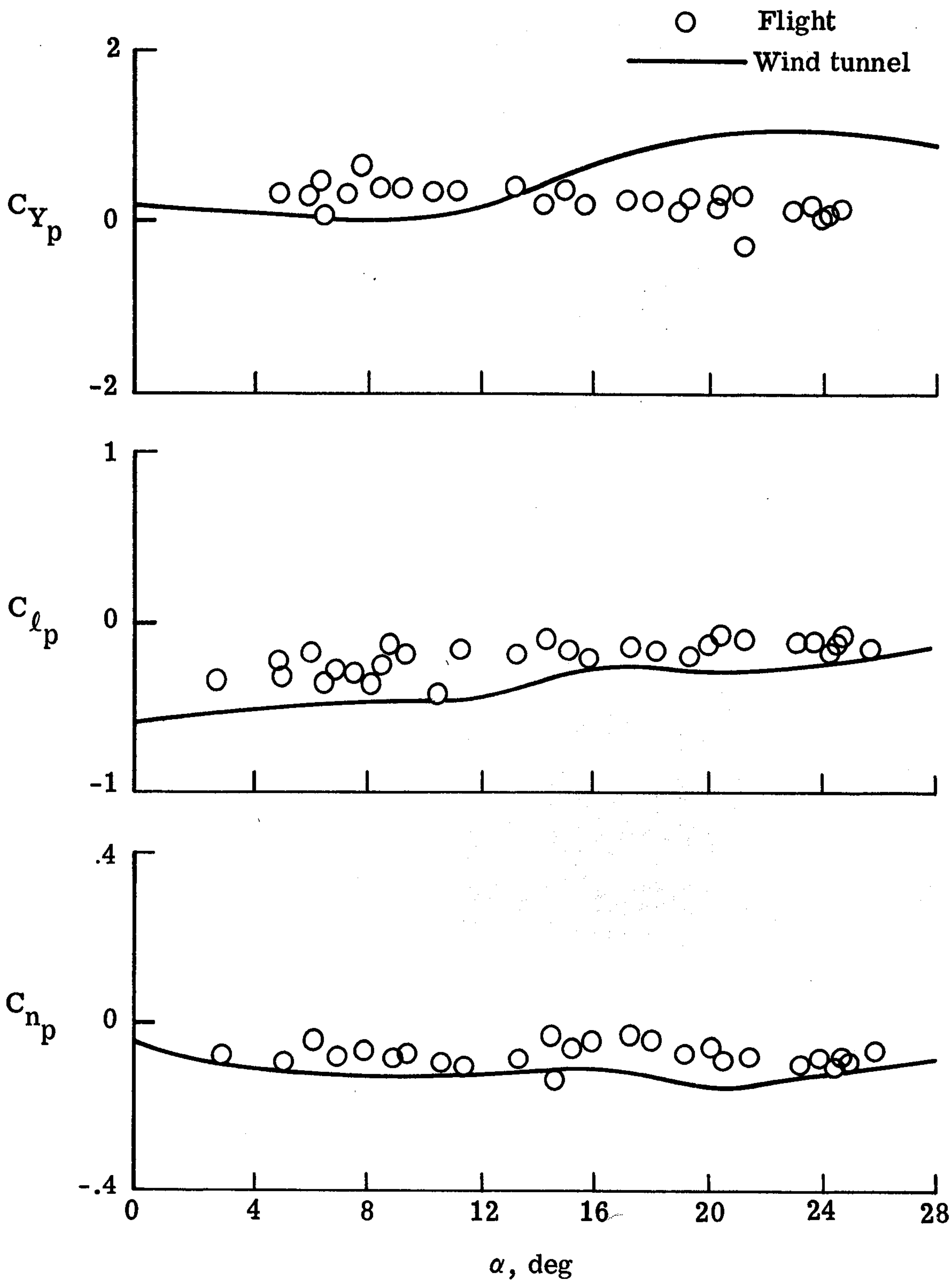


Figure 19.- Comparison of roll-rate derivatives determined from flight and wind tunnel.

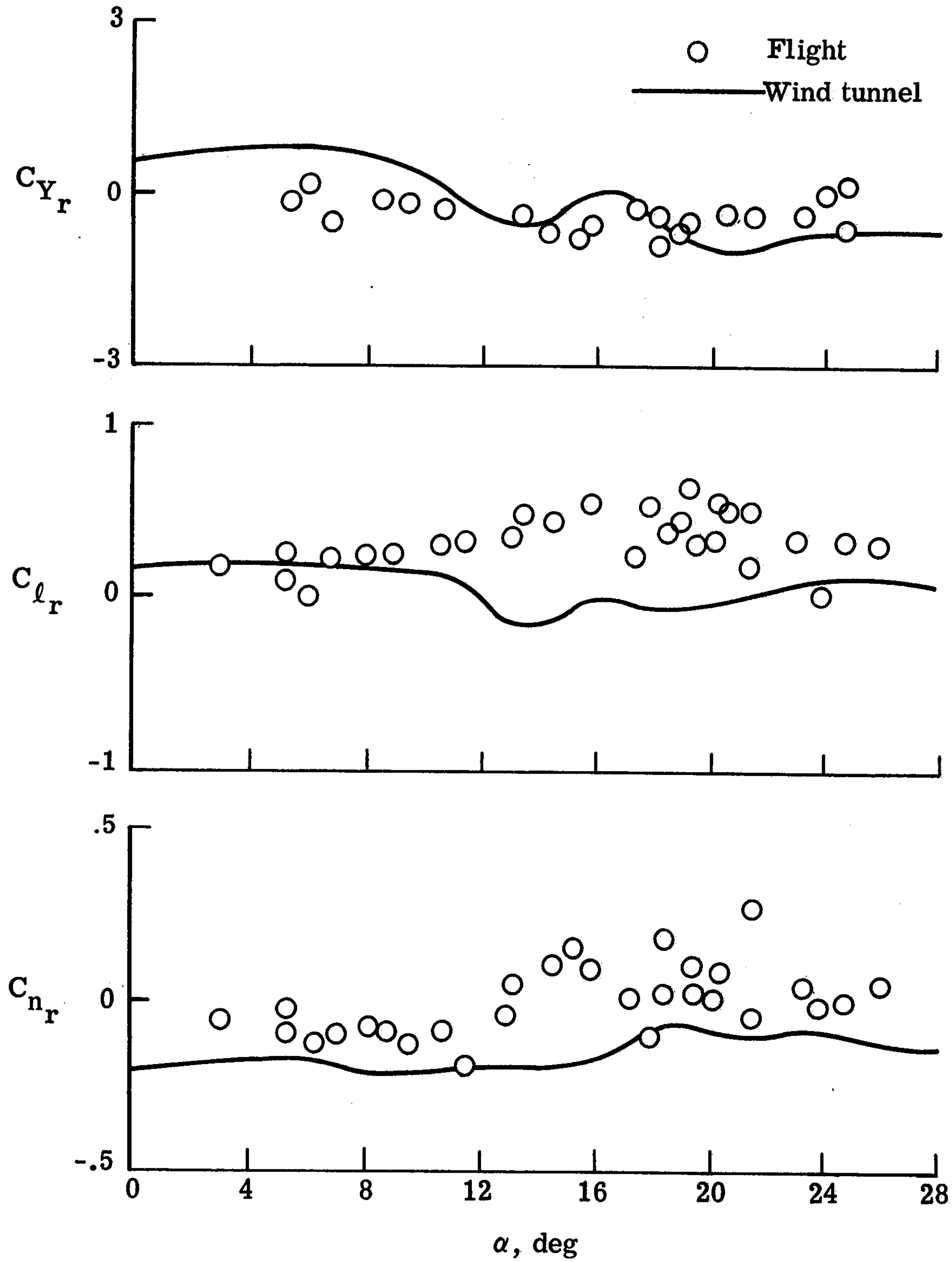


Figure 20.- Comparison of yaw-rate derivatives determined from flight and wind tunnel.

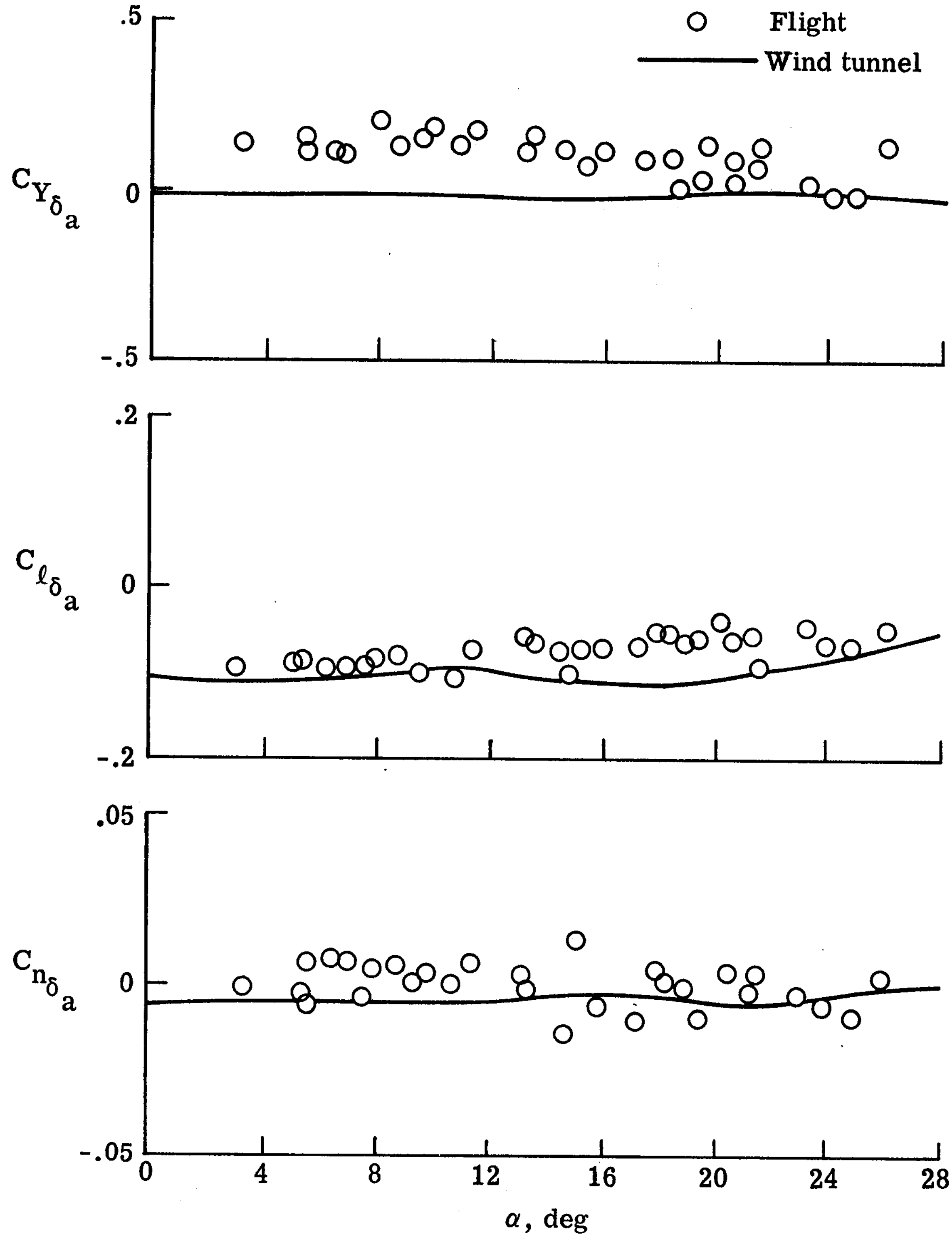


Figure 21.- Comparison of aileron derivatives determined from flight and wind tunnel.

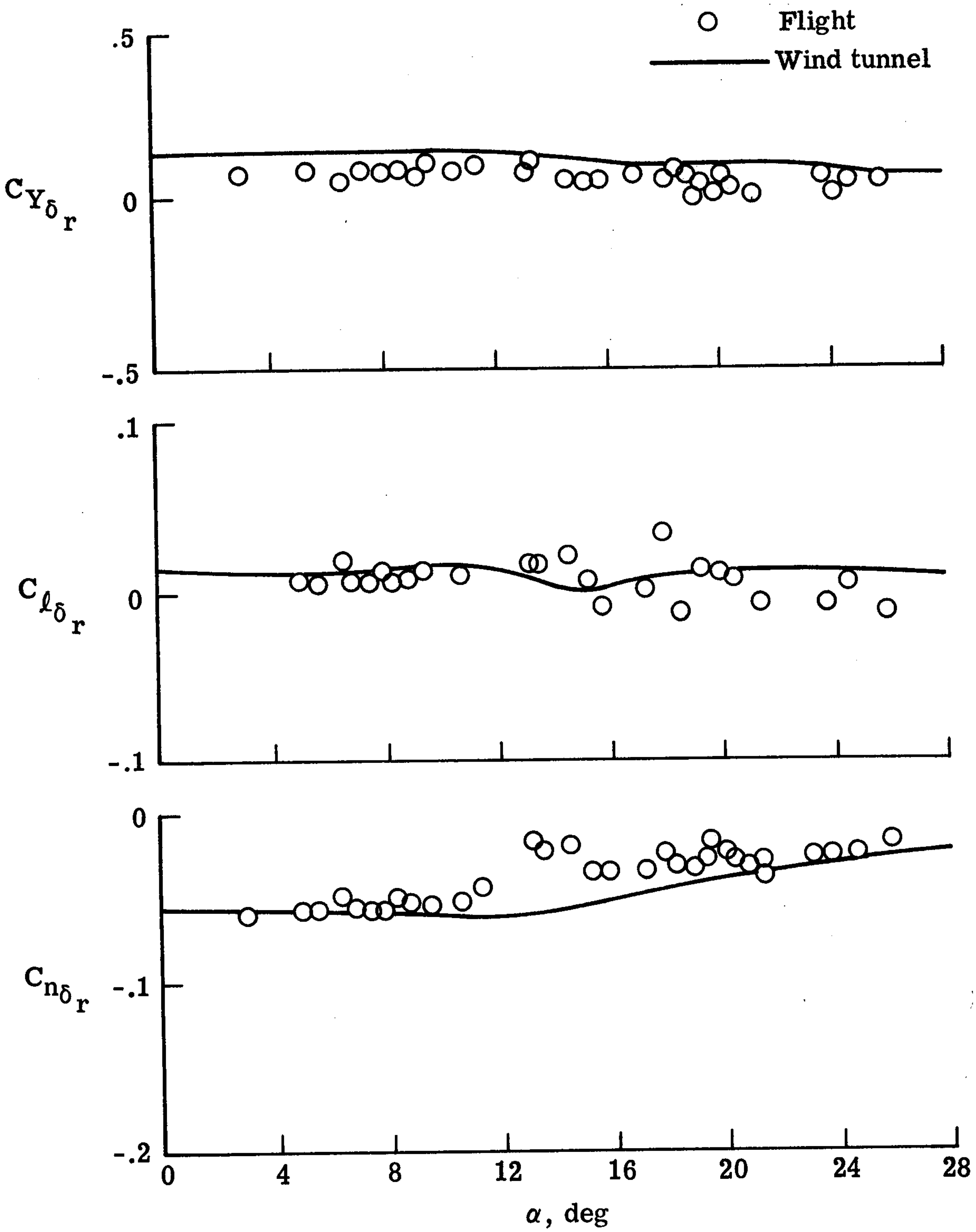


Figure 22.- Comparison of rudder derivatives determined from flight and wind tunnel.

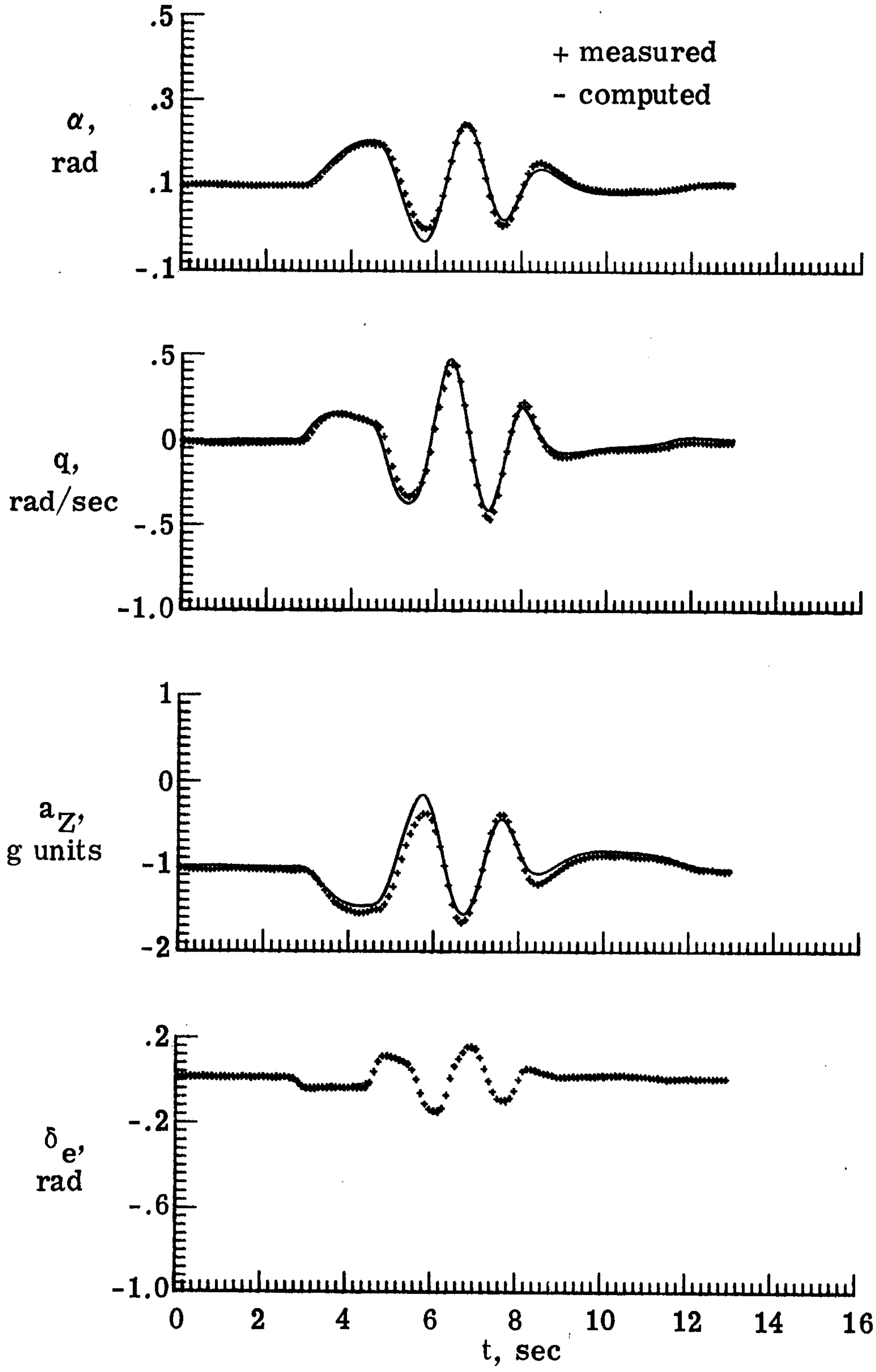


Figure 23.- Measured longitudinal flight data time histories and those computed by using parameters obtained by stepwise regression method.

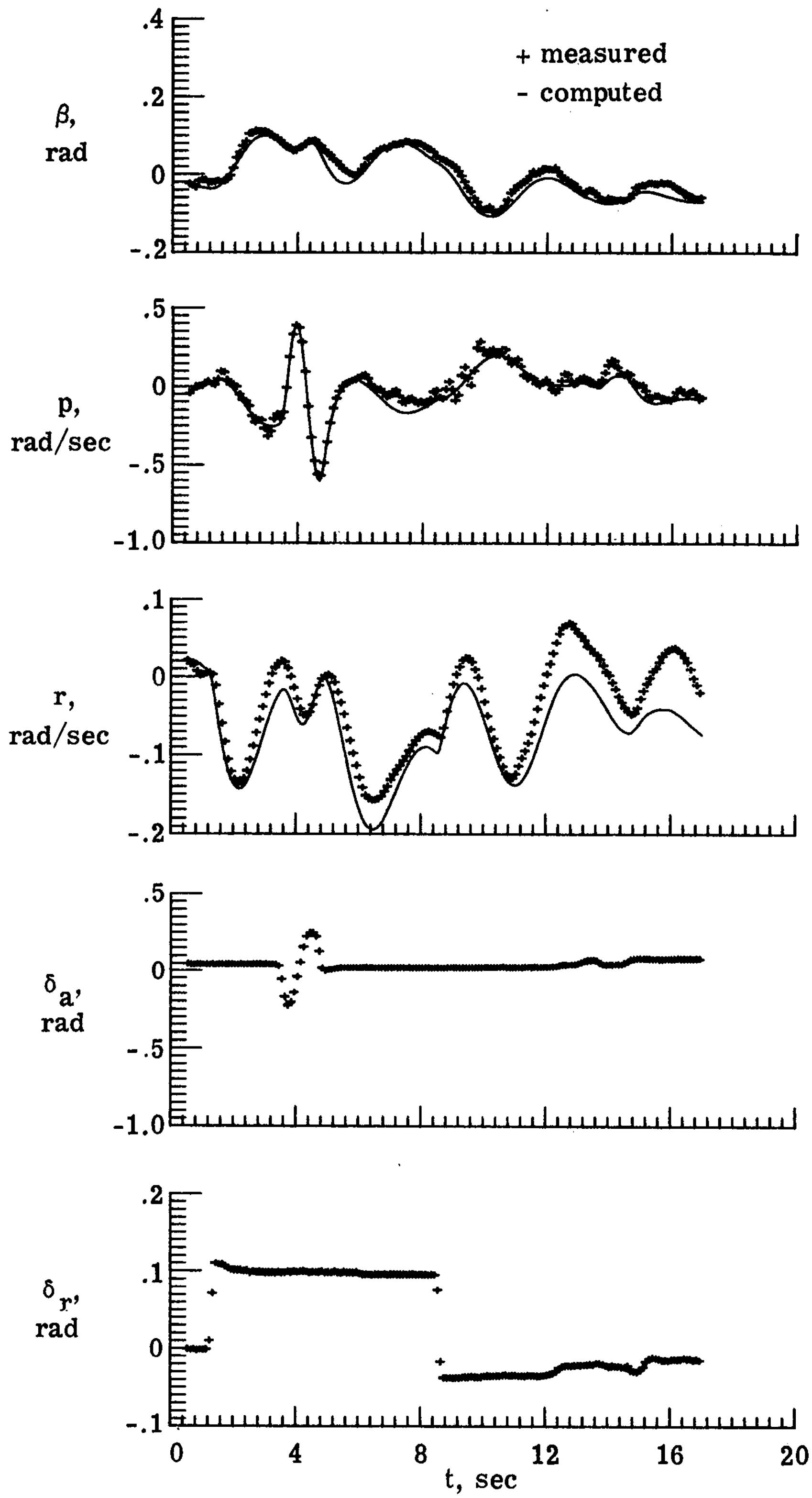


Figure 24.- Measured lateral flight data time histories and those computed by using parameters obtained by stepwise regression method.

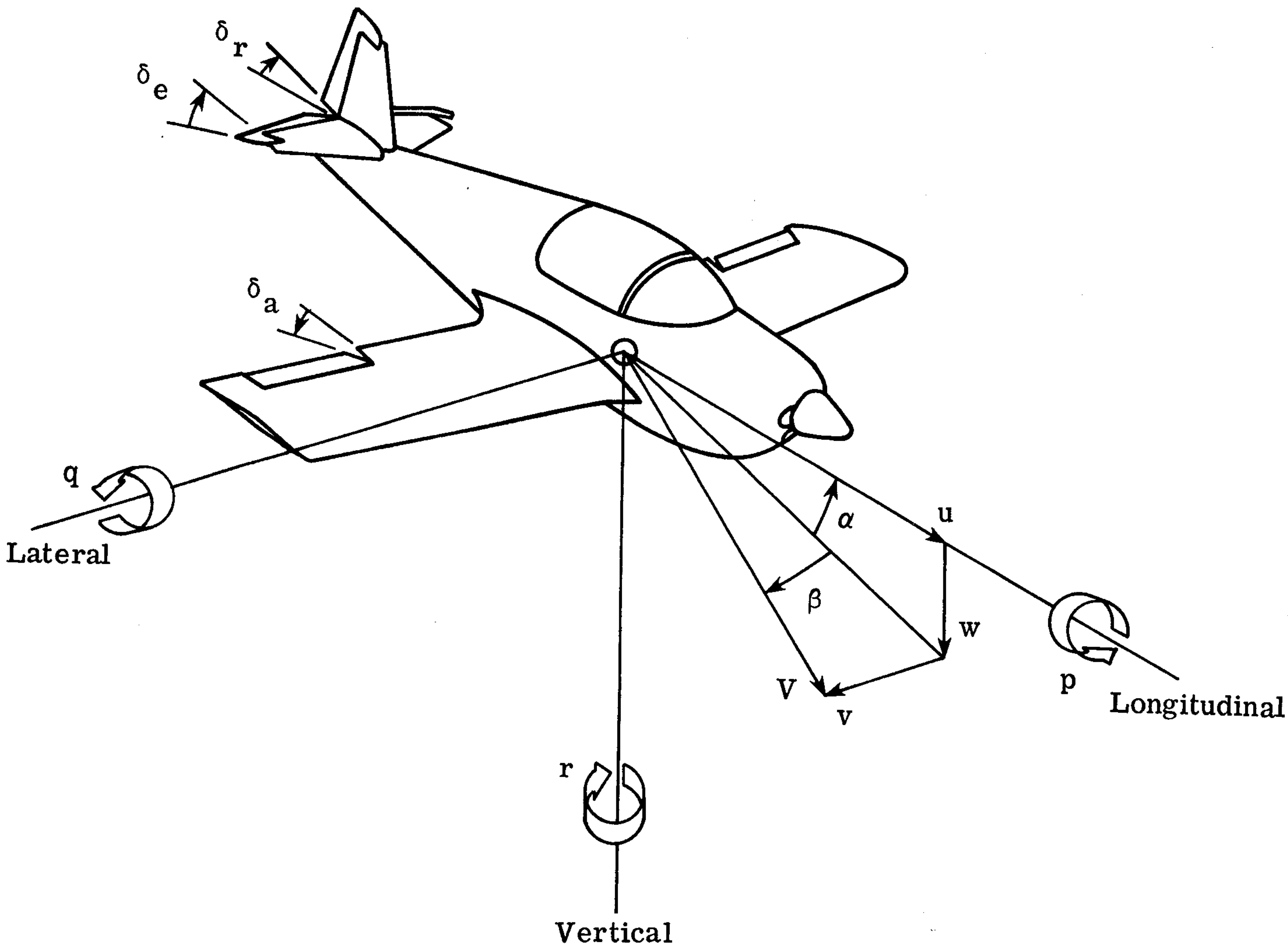


Figure 25.- Body system of axes. Arrows indicate positive direction of quantities.

| 1. Report No. | 2. Government Accession No. | 3. Recipient's Catalog No. |
|---|---|---|
| NASA TM-84635 | | |

| 4. Title and Subtitle | |
|---|---|
| Determination of Stability and Control Parameters of a General Aviation Airplane from Flight Data. | 5. Report Date<br>March 1983 |
| | 6. Performing Organization Code<br>505-34-03-06 |
| 7. Author(s)<br>*Imran Abbasy | 8. Performing Organization Report No. |
| 9. Performing Organization Name and Address<br>NASA Langley Research Center<br>Hampton, VA 23665 | 10. Work Unit No. |
| | 11. Contract or Grant No. |
| 12. Sponsoring Agency Name and Address<br>National Aeronautics and Space Administration<br>Washington, DC 20546 | 13. Type of Report and Period Covered<br>Technical Memorandum |
| | 14. Sponsoring Agency Code |

15. Supplementary Notes

*The George Washington University, Joint Institute for Advancement of Flight Sciences, NASA Langley Research Center, Hampton, Virginia.

16. Abstract

Values for the stability and control parameters for a general aviation airplane have been determined from flight data. Lateral and longitudinal transient maneuvers were analyzed by the equation error and output error methods. There was a good agreement between the parameters extracted from flight data and those predicted by wind tunnel.

| 17. Key Words (Suggested by Author(s)) | 18. Distribution Statement |
|---|---|
| General aviation<br>Stepwise regression<br>Maximum likelihood<br>System identification<br>STAR Category - 08 | Unclassified - Unlimited<br><br>Subject Category 08 |

| 19. Security Classif. (of this report) | 20. Security Classif. (of this page) | 21. No. of Pages | 22. Price* |
|---|---|---|---|
| Unclassified | Unclassified | 44 | A03 |

N-305

For sale by the National Technical Information Service, Springfield, Virginia 22161